

Final Summary Report of the Research Project (ERB, 624732):

Introduction: Birds represent one of the most remarkable radiations in the history of life. The origin of flight and the diversification of birds have become classic ‘textbook’ examples for discussions about evolutionary models, biomechanics, the history of life, and phylogenetics. Much attention has focused on the discovery and description of new fossils, both derived theropods and basal birds: in particular, sediments of the Jehol Group in Liaoning and other provinces in China have doubled the number of Mesozoic bird taxa and have considerably expanded our knowledge of derived theropod dinosaurs. All this wealth of fossil data and new phylogenetic studies have established the relationships of basal bird groups, as well as their phylogenetic nesting among theropod dinosaurs, with dromaeosaurid and troodontid theropods as their closest sister groups. The mode and tempo of avian evolution have received much attention in recent years, thanks to the assembly of more complete datasets, the ongoing flow of new specimens and taxa, and the development of new techniques of macroevolutionary analysis. Recent studies revealed an avian radiation characterized by the gradual acquisition of apomorphies followed by accelerated (yet clade heterogeneous) rates of evolution. However, in the context of Coelurosauria (a diverse clade including *T. rex* and its kin, the ostrich-mimic ornithomimosaur, and the sickle-clawed dromaeosaurids, among others), previous analyses have considered the skeleton as a whole, apart from studies focusing on single continuous traits. Here, I document the evolutionary dynamics of each anatomical region of the coelurosaurian skeleton. I aim at disentangling the relative role of each body part in the evolutionary dynamics of Coelurosauria. In doing so, I have the goal of resolving the timing of the origin and acquisition of key evolutionary novelties during the evolution of Avialae (birds) and closely related theropod dinosaurs and identifying the crucial characters in driving the initial (and subsequent) radiation(s) of birds

Results

1. When considered as a whole, the cranium (Figs. 1-5) of coelurosaurian dinosaurs displayed accelerated evolutionary rates at the base of tyrannosauroids (also among derived members of the clade), alvarezsaurids, oviraptorosaurs, and paravians. Significantly low rates were present in the more derived dromaeosaurid and troodontid paravians. Cranial morphological disparity increased over time for the entire coelurosaurian clade, particularly after the Santonian. In the disparity morphospace, tyrannosauroids and oviraptorosaurs cluster apart from other groups and in opposite regions of the morphospace, reflecting their derived cranial anatomy. The tyrannosauroid cranium is also remarkable in being much more disparate than that of the other coelurosaurians, including birds.
2. In the neurocranium (the skull area that protects the brain and associated neuronal structures; Figs. 6-10), only derived tyrannosauroids displayed higher rates of evolution. Over time, neurocranial disparity remained relatively steady (with a dip in the Berriasian-Valanginian) until the Santonian; subsequently, this area of the skull experienced a remarkable surge in disparity. Tyrannosauroids are set apart from other coelurosaurians by occupying more than half of morphospace. These theropods show a greater disparity than all other coelurosaurians.
3. The facial skeleton (Fig. 11-15) showed accelerated rates in derived tyrannosauroids and in the earliest stages of the evolution of paravian theropods. In contrast, slower evolutionary rates appeared among derived dromaeosaurid theropods. Over time, the facial elements of the coelurosaurian skull experienced a decrease in disparity from the Kimmeridgian to the Aptian; subsequently, this region experienced a remarkable increase in diversity that culminated in the Maastrichtian. In the disparity

morphospace, paravians, therizinosauroids and alvarezsaurids are restricted to a relatively small region, whereas tyrannosauroids spread over nearly half of the morphospace. This is consistent with the finding of a greater facial disparity in tyrannosauroids than in other coelurosaurians.

4. The coelurosaurian mandible (Figs. 16-20) displayed accelerated evolutionary rates at the base of alvarezsaurids and oviraptorosaurs, and in a few bird species and the most derived tyrannosaurids. Since the Late Jurassic, the mandible increased in disparity, slowly until the Albian but rapidly after this geological stage. In terms of morphospace occupation, mandibular disparity appears restricted to one fourth of that shape space in paravians, ornithomimosaurs and compsognathids; tyrannosauroids and oviraptorosaurs, in contrast, occupy very different regions of the morphospace. Again, tyrannosauroids are the most disparate coelurosaurs in mandibular morphology, in this case followed by birds, therizinosauroids, and oviraptorosaurs.
5. Significantly higher rates of dental evolution (Fig. 21) were found in early ornithomimosaurs; no significantly different (whether higher or lower) rates were present in other clades. Over time, dental disparity increased in Coelurosauria; most of this increase took place from the Tithonian to the Barremian. Subsequently, dental disparity experienced very little variation. Paravian dental disparity appears widespread in the morphospace, with substantial overlap among troodontids, dromaeosaurids and birds. Tyrannosauroids, alvarezsaurids and birds became more disparate than other coelurosaurians in tooth morphology.
6. Considering the postcranium as a whole (Fig. 26-30), accelerated rates of evolution took place at the base of Maniraptora and at the base of maniraptoran clades like therizinosauroids, alvarezsaurids, and paravians (notably also in birds). Such high rates are widespread among numerous bird lineages. Significantly low rates are present among maniraptoran outgroups such as ornithomimids and also within some dromaeosaurid paravians. Postcranial disparity increased through time until the Campanian, with two remarkable dips during the Berriasian-Valanginian and the Albian. In terms of morphospace occupation, birds occupy the largest area and appear distinct from all other coelurosaurians. Disparity is highest in birds, followed by tyrannosauroids and alvarezsaurids.
7. The coelurosaurian axial skeleton (Fig. 31-35) showed accelerated evolutionary rates at the base of alvarezsaurids and lower rates in some early dromaeosaurid paravians. The axial skeleton displayed a gradual increase in disparity until the Campanian, decreasing subsequently during the Maastrichtian. Birds achieved the greatest axial disparity among Coelurosauria, followed by oviraptorosaurs and tyrannosauroids. Birds and tyrannosauroids appear segregated from other coelurosaurians in the disparity morphospace, with all other clades largely occupying overlapping positions.
8. In the pectoral girdle (Figs. 36-40), higher evolutionary rates are present at the base of Paraves and several bird lineages. Throughout time, pectoral disparity experienced surge from the Berriasian to the Aptian; subsequently, it remain relatively constant until the end of the Maastrichtian, except for a dip in the Coniacian-Santonian. Birds, and to a lesser degree oviraptorosaurs and tyrannosauroids, evolved the most disparate pectoral girdles among coelurosaurians. All paravians occupy a distinct half of the morphospace than the other coelurosaurians, with birds clearly segregated from the other paravian subclades.
9. The forelimb (Figs. 41-45) experienced accelerated rates of evolution ancestrally in alvarezsaurids and among derived bird lineages. Over time, forelimb disparity greatly increased from the Kimmeridgian to the Aptian; subsequently forelimb disparity fluctuated until the Campanian, slightly decreasing during the Maastrichtian. Birds,

tyrannosauroids and ornithomimosaurids occupy different regions of the disparity morphospace relative to the position of the other coelurosaurian clades. Again, birds display the greatest disparity in this anatomical region, followed by alvarezsaurids and tyrannosauroids.

10. The pelvic girdle (Figs. 46-50) shows accelerated evolutionary rates ancestrally in Maniraptora, Oviraptorosauria+Paraves, and Paraves. Throughout time, this anatomical region generally became more disparate until the Santonian, with an extreme dip in the Barresian-Valanginian and decrease in disparity during the Campanian and Maastrichtian. There is relatively little overlap in morphospace occupation for most coelurosaurian clades, indicating the disparate pelvic morphologies evolved by these groups, more so than in other anatomical regions. Disparity was particularly higher in birds, tyrannosauroids and therizinosauroids.
11. In the hindlimb (Figs. 51-55), paravians and this clade plus oviraptorosaurs showed accelerated evolutionary rates ancestrally. Notably, various bird lineages also display significantly higher rates. The disparity morphospace is characterized by having birds, comosognathids, and tyrannosauroids occupying different regions than other coelurosaurians. Over time, the hindlimb experienced a two-phase increase disparity: one from the Barremian to the Aptian and a large surge from the Albian to the Santonian. This anatomical region shows then a decrease in disparity during the Campanian and Maastrichtian. Birds, alvarezsaurids, therizinosauroids and tyrannosauroids show all the greatest disparity recorded among Coelurosauria.
12. These results highlight the important role in the postcranium in the evolution of birds, with a particular focus on limb module evolution in the transition to flight. All postcranial regions in Avialae display greater disparity than in most other clades. Overall, these postcranial regions increase in disparity during the Late Jurassic and most of the Cretaceous, all of them showing a post-Santonian disparity decrease. In the avian cranium, significantly higher rates of evolution are found in the facial skeleton.

Impact: These results represent the most comprehensive and detailed study of morphological evolutionary dynamics in coelurosaurian dinosaurs, including birds and their closest relatives. This study allows us to understand the relative influence of each anatomical region of the coelurosaurian skeleton in the macroevolution of the clade, particularly the relative role of each body part in the accelerated rates of evolution previously reported in early avian theropods. The results of the project will form the foundation for future analyses seeking to disentangle the role of particular traits in the radiation of birds from coelurosaurian theropods, from a functional, morphological and phylogenetic perspective.

Figure 1. Rates of morphological evolution based on the entire cranial characters in coelurosaurian theropods. The proportion of significantly high (red) and significantly low (blue) per-branch rates based on 100 dating replications are illustrated with pie charts.

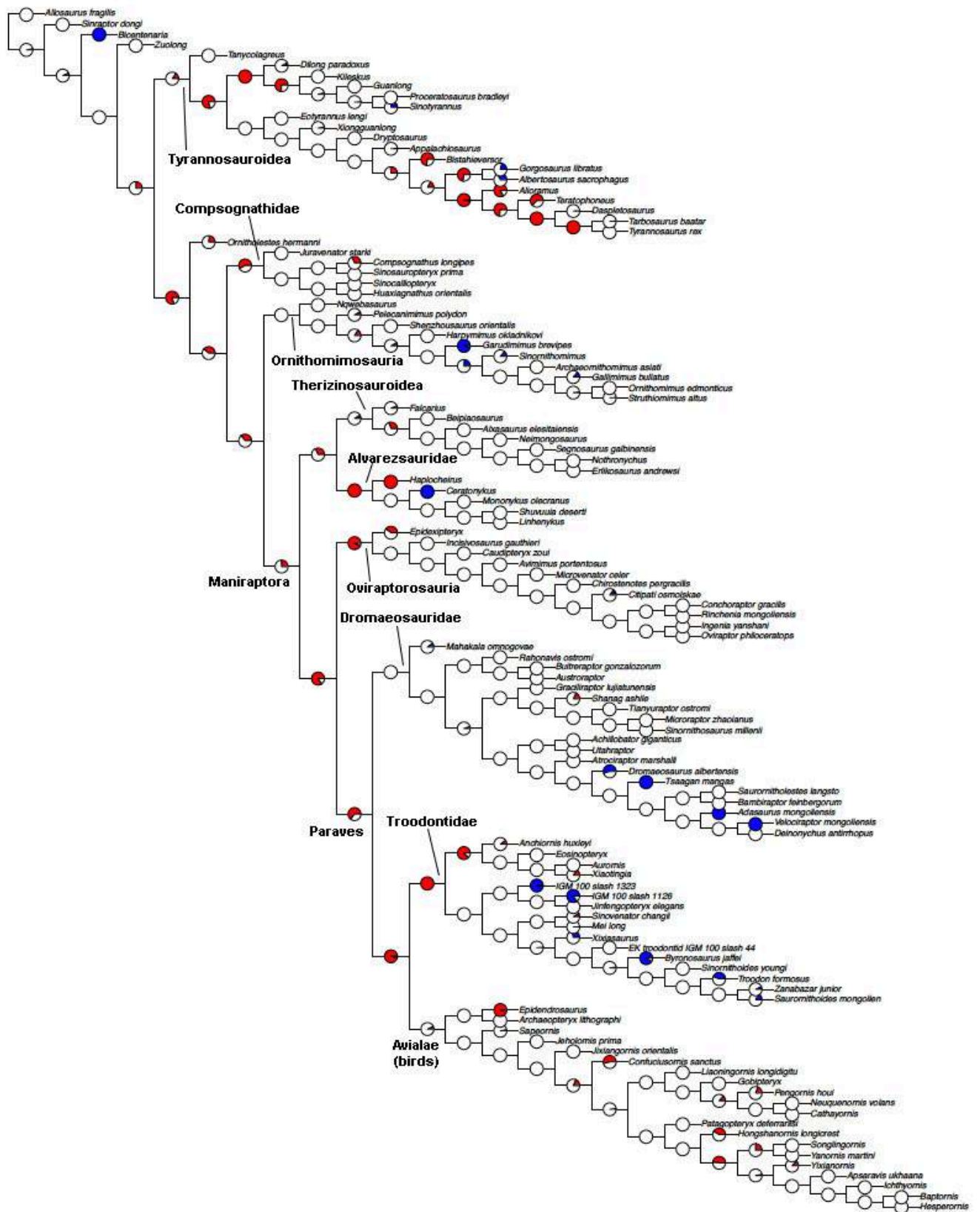


Figure 2. Disparity morphospace resulting from Principal Coordinate Analysis (PCO) for the entire cranium in various coelurosaurian clades. Black squares = Tyrannosauroidae; blue asterisks = Compsognathidae; empty circles = Ornithomimosauria; blue crosses = Alvarezsauridae; pink solid circles = Oviraptorosauria; green rhombs = Therizinosauria; empty red triangles pointing up = Dromaeosauridae; empty red triangles pointing down = Troodontidae; red solid triangles = Avialae (birds).

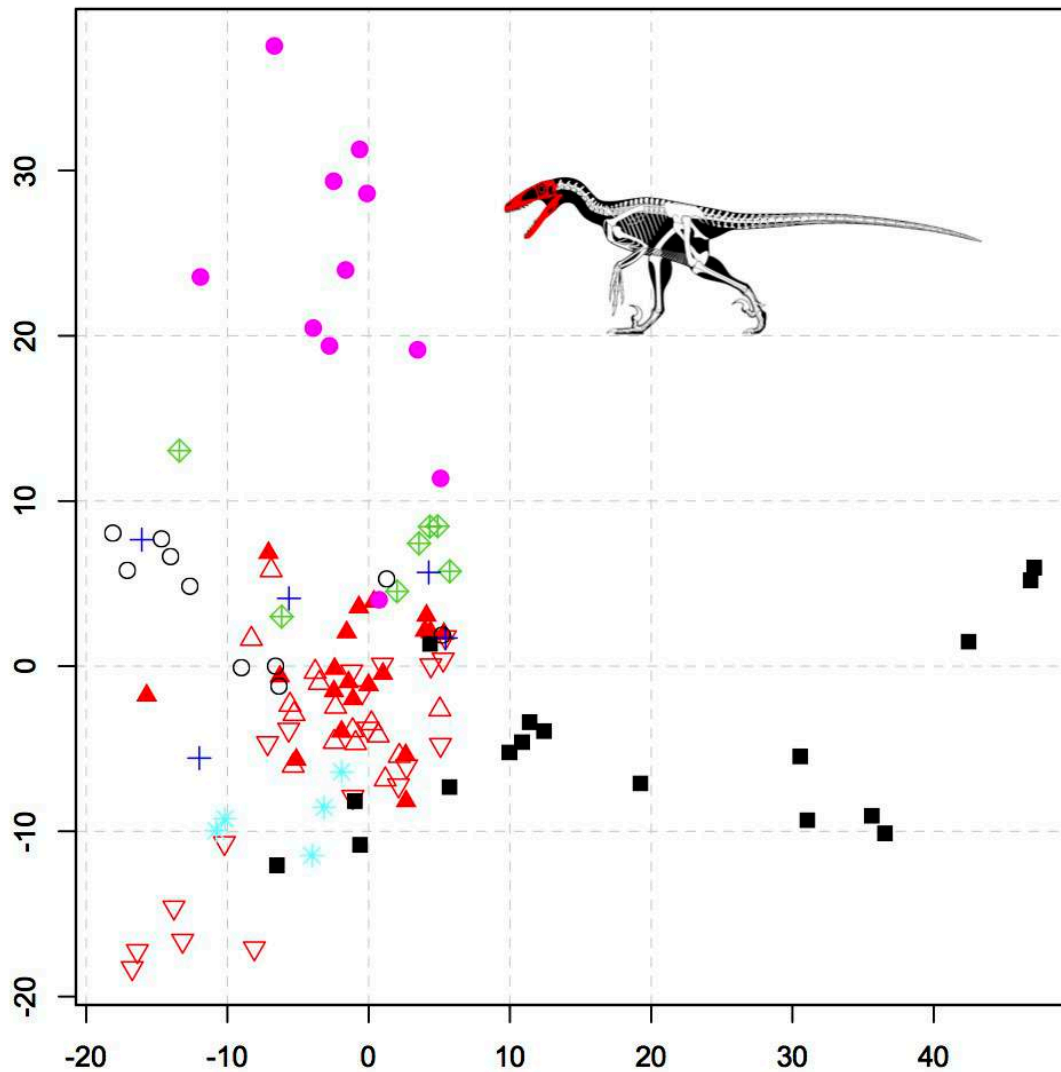


Figure 3. Cranial disparity results based on taxa binned by clade. Disparity values based on the weighted mean pairwise disparity (WMPD) from the generalised Euclidean distance matrix (GED). 95% confidence intervals based on 10,000 bootstrap replicates are also plotted.

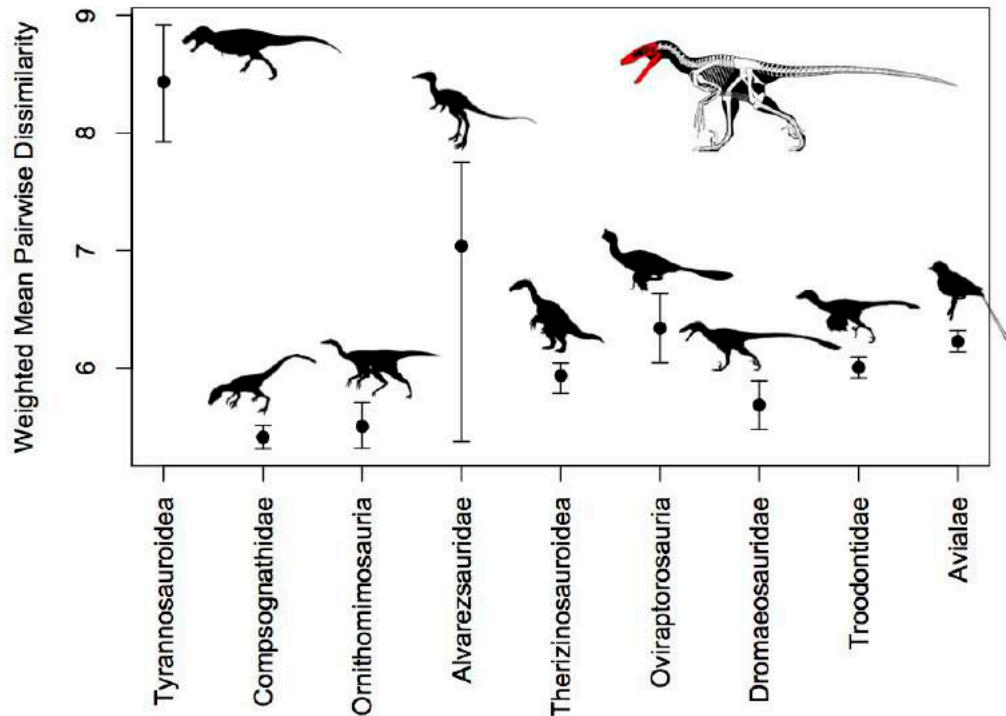


Figure 4. Cranial disparity results based on taxa binned by clade. Disparity values based on the weighted mean pairwise disparity (WMPD) from the sum of variances from PCO scores. 95% confidence intervals based on 10,000 bootstrap replicates are also plotted.

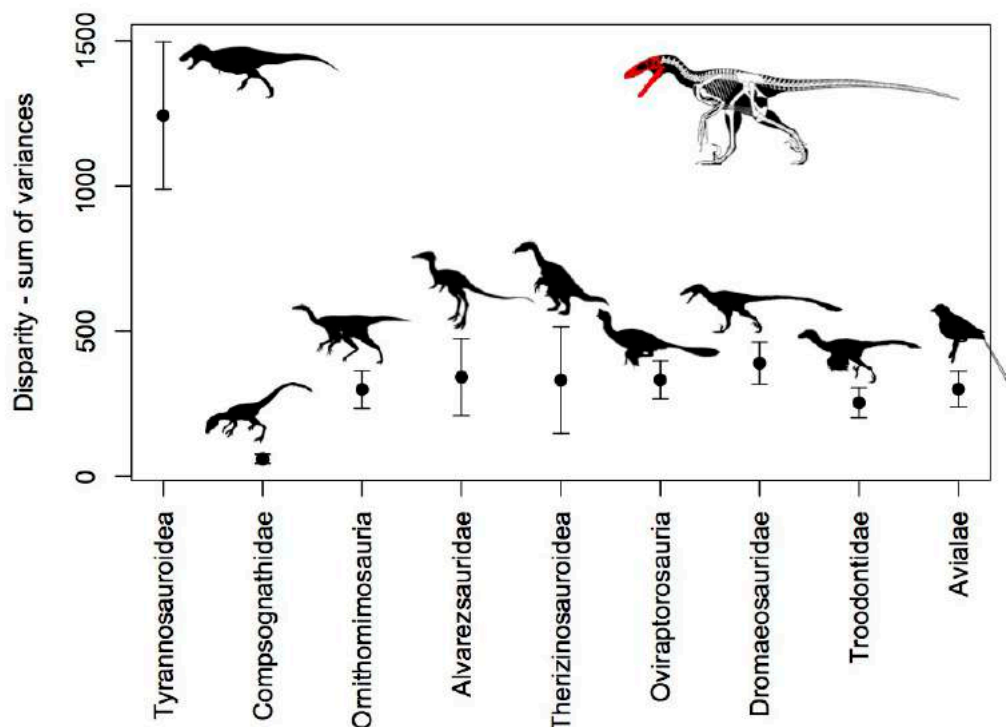


Figure 5. Temporal disparity trend of the entire cranium in coelurosaurian theropods.

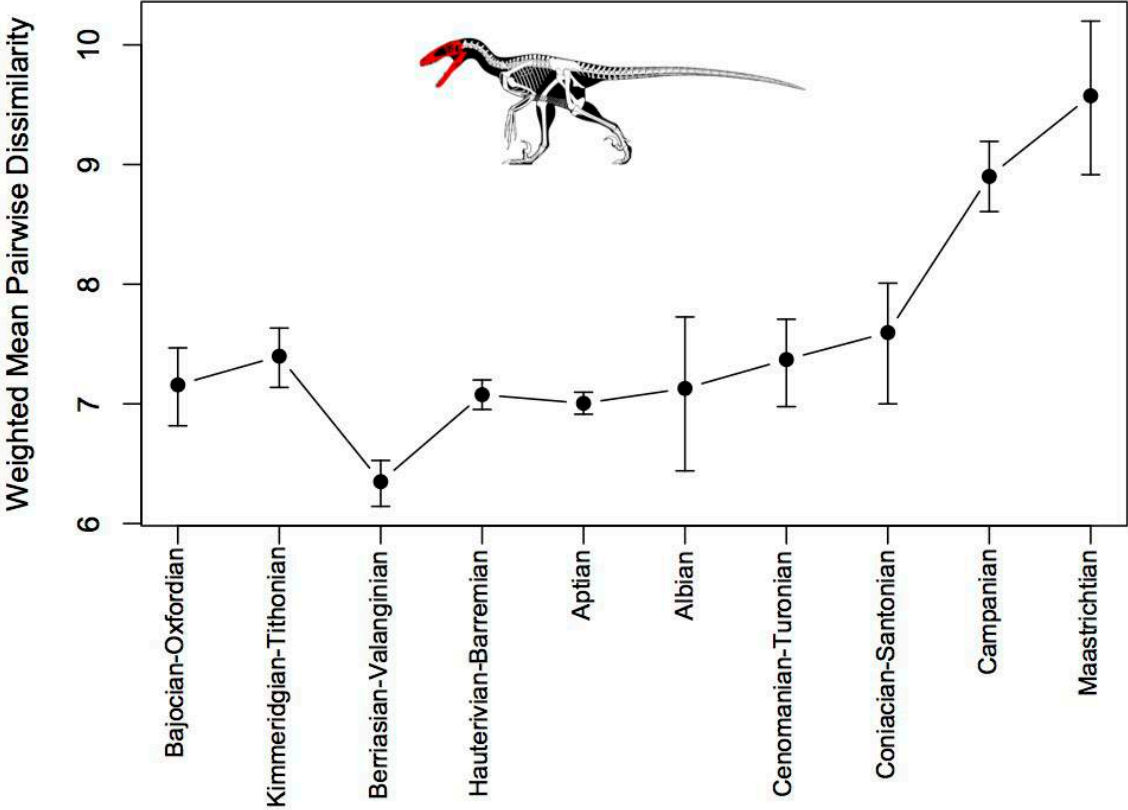


Figure 6. Rates of morphological evolution based on neurocranial characters in coelurosaurian theropods. The proportion of significantly high (red) and significantly low (blue) per-branch rates based on 100 dating replications are illustrated with pie charts.

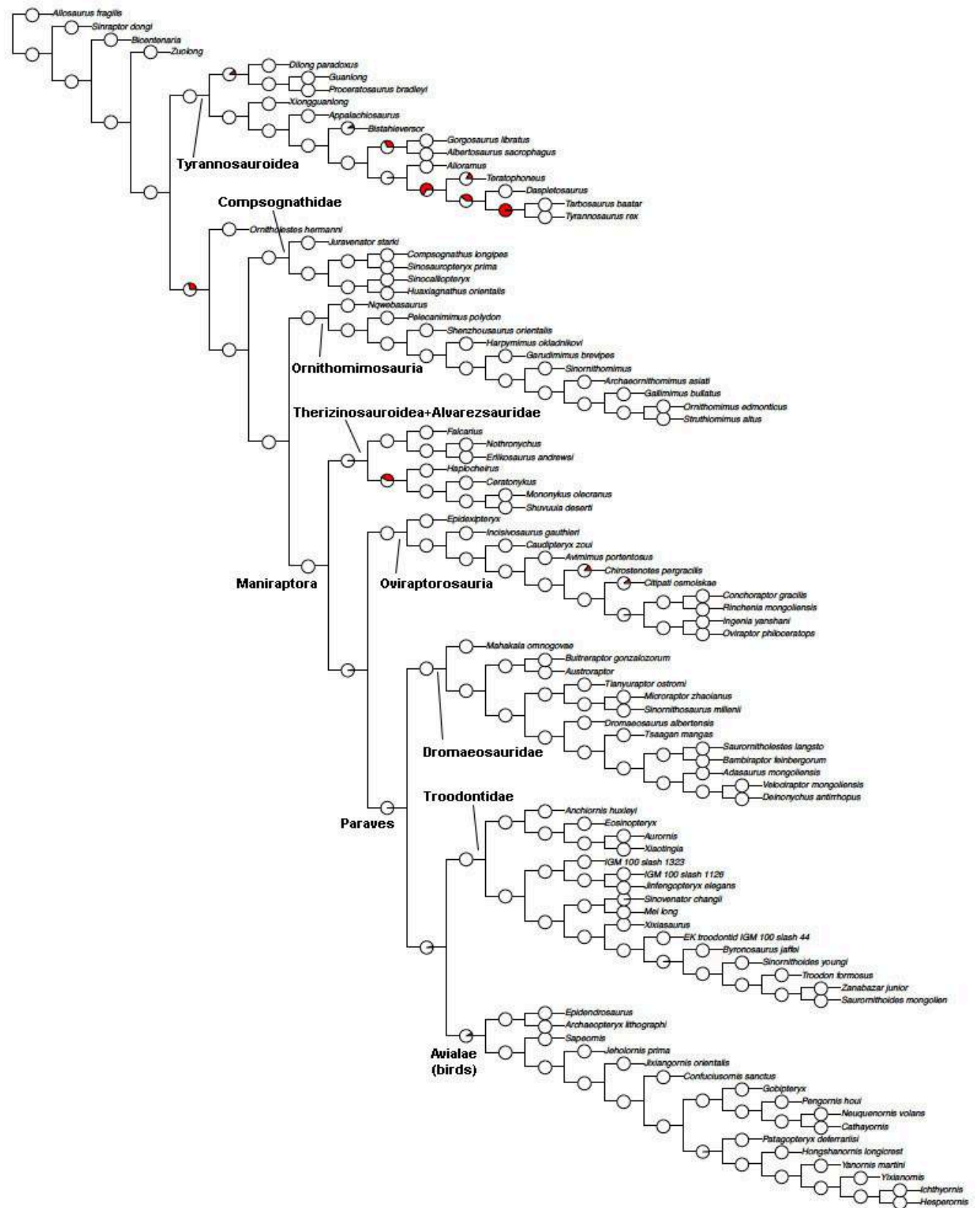


Figure 7. Neurocranial disparity morphospace resulting from Principal Coordinate Analysis (PCO) for the entire cranium in various coelurosaurian clades. Black squares = Tyrannosauroidae; blue asterisks = Compsognathidae; empty circles = Ornithomimosauria; blue crosses = Alvarezsauridae; pink solid circles = Oviraptorosauria; green rhombs = Therizinosauria; empty red triangles pointing up = Dromaeosauridae; empty red triangles pointing down = Troodontidae; red solid triangles = Avialae (birds).

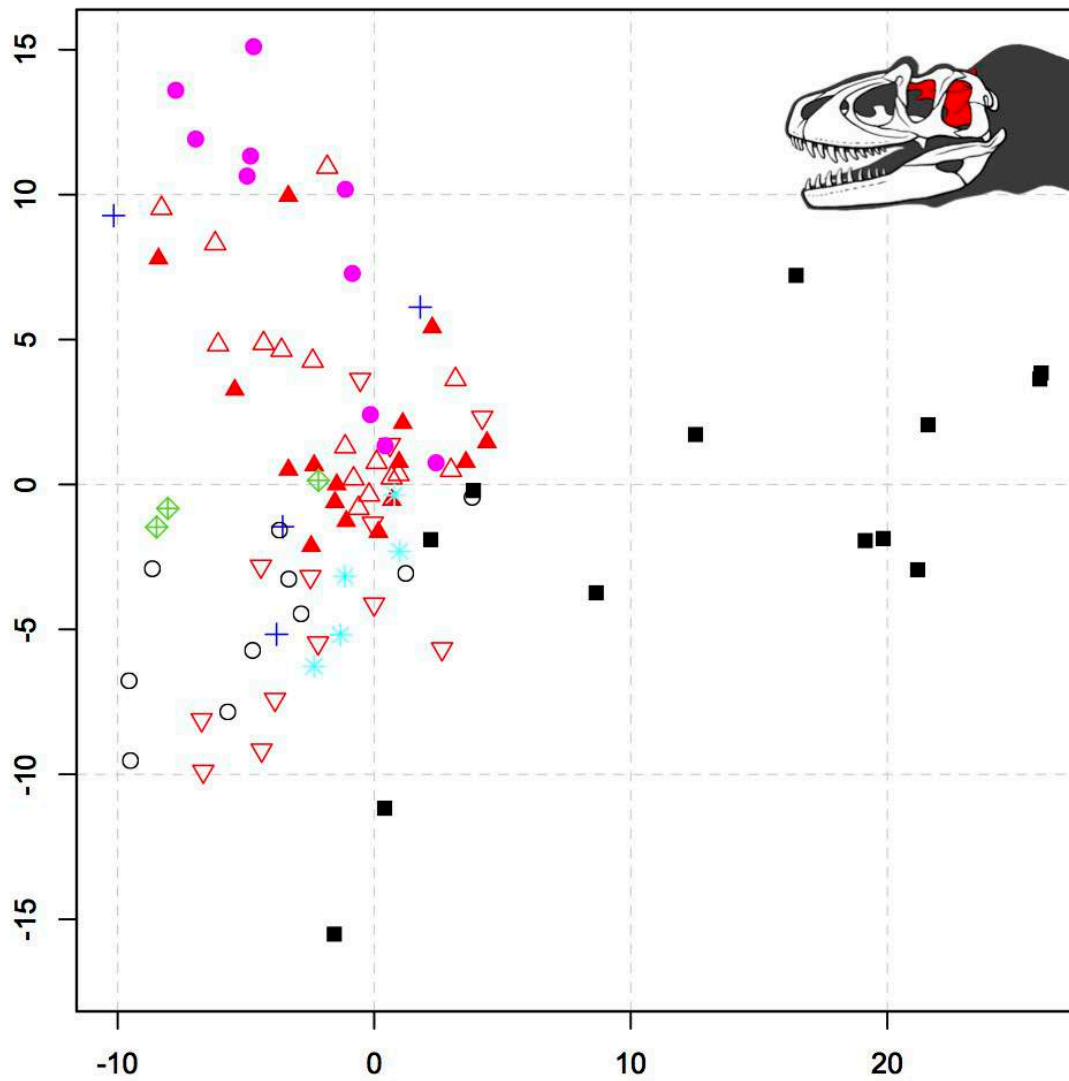


Figure 8. Neurocranial disparity results based on taxa binned by clade. Disparity values based on the weighted mean pairwise disparity (WMPD) from the generalised Euclidean distance matrix (GED). 95% confidence intervals based on 10,000 bootstrap replicates are also plotted.

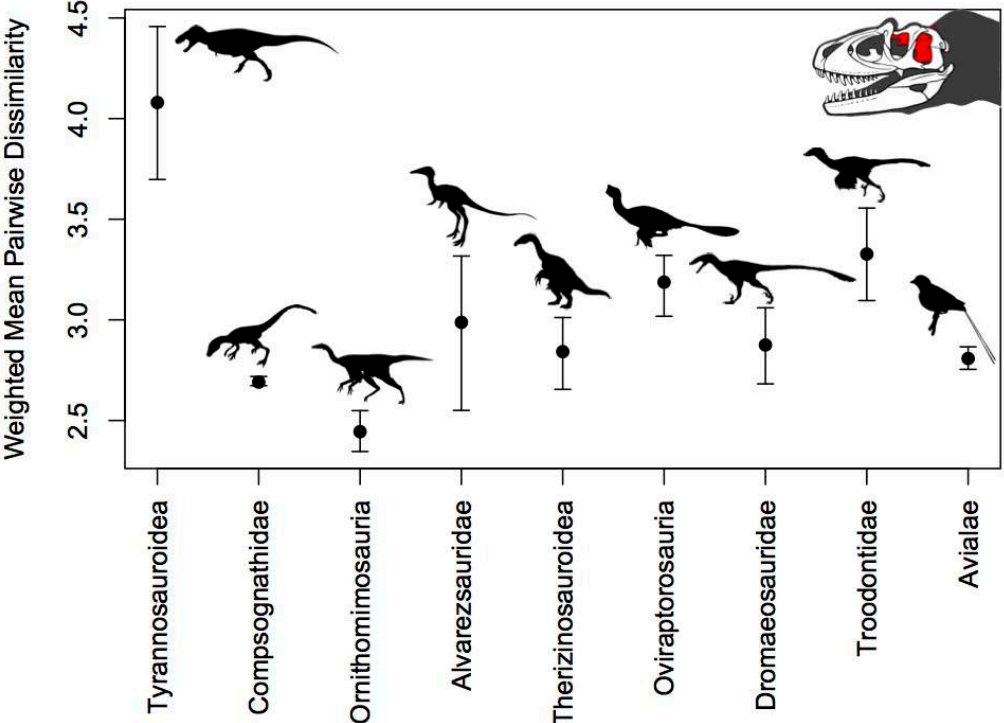


Figure 9. Neurocranial disparity results based on taxa binned by clade. Disparity values based on the weighted mean pairwise disparity (WMPD) from the sum of variances from PCO scores. 95% confidence intervals based on 10,000 bootstrap replicates are also plotted.

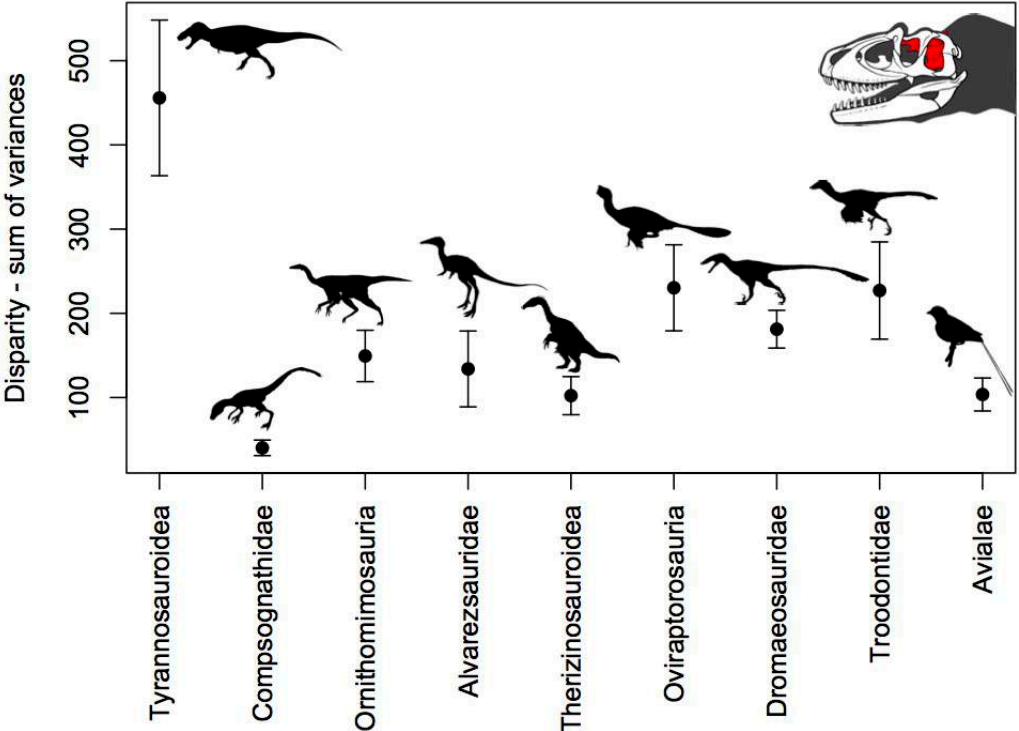


Figure 10. Temporal disparity trend of the neurocranium in coelurosauria theropods.

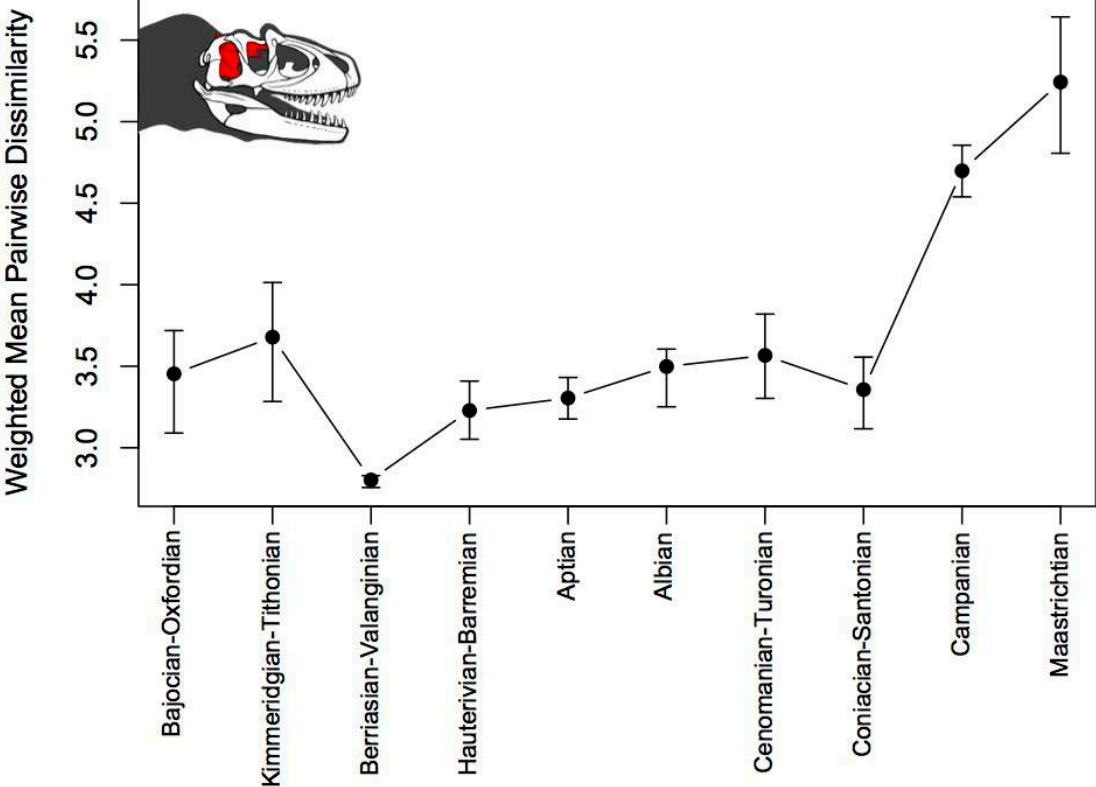


Figure 11. Rates of morphological evolution based on facial characters in Coelurosauria. The proportion of significantly high (red) and significantly low (blue) per-branch rates based on 100 dating replications are illustrated with pie charts.

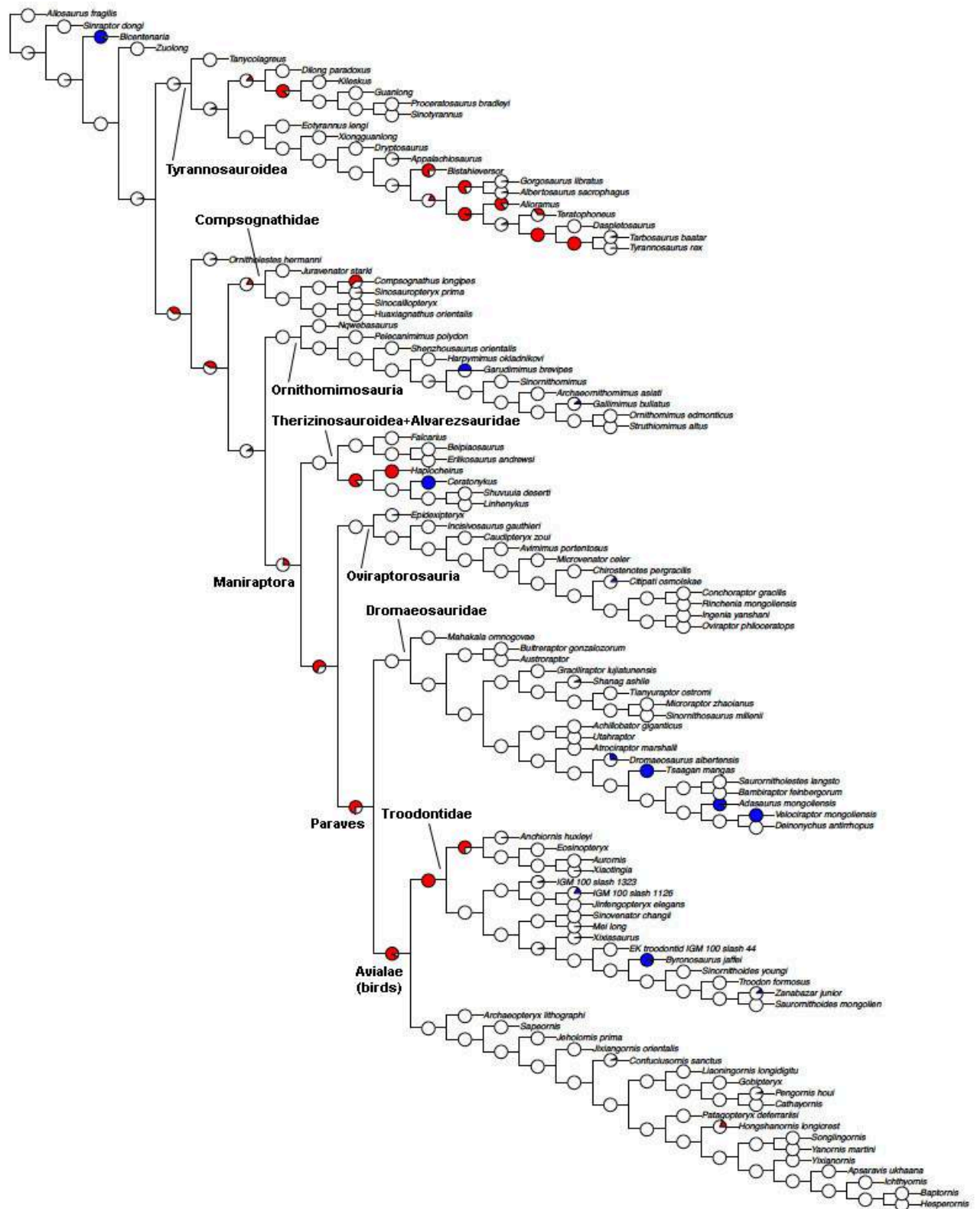


Figure 12. Disparity morphospace resulting from Principal Coordinate Analysis (PCO) for the facial skeleton in various coelurosaurian clades. Black squares = Tyrannosauroidae; blue asterisks = Compsognathidae; empty circles = Ornithomimosauria; blue crosses = Alvarezsauridae; pink solid circles = Oviraptorosauria; green rhombs = Therizinosauria; empty red triangles pointing up = Dromaeosauridae; empty red triangles pointing down = Troodontidae; red solid triangles = Avialae (birds).

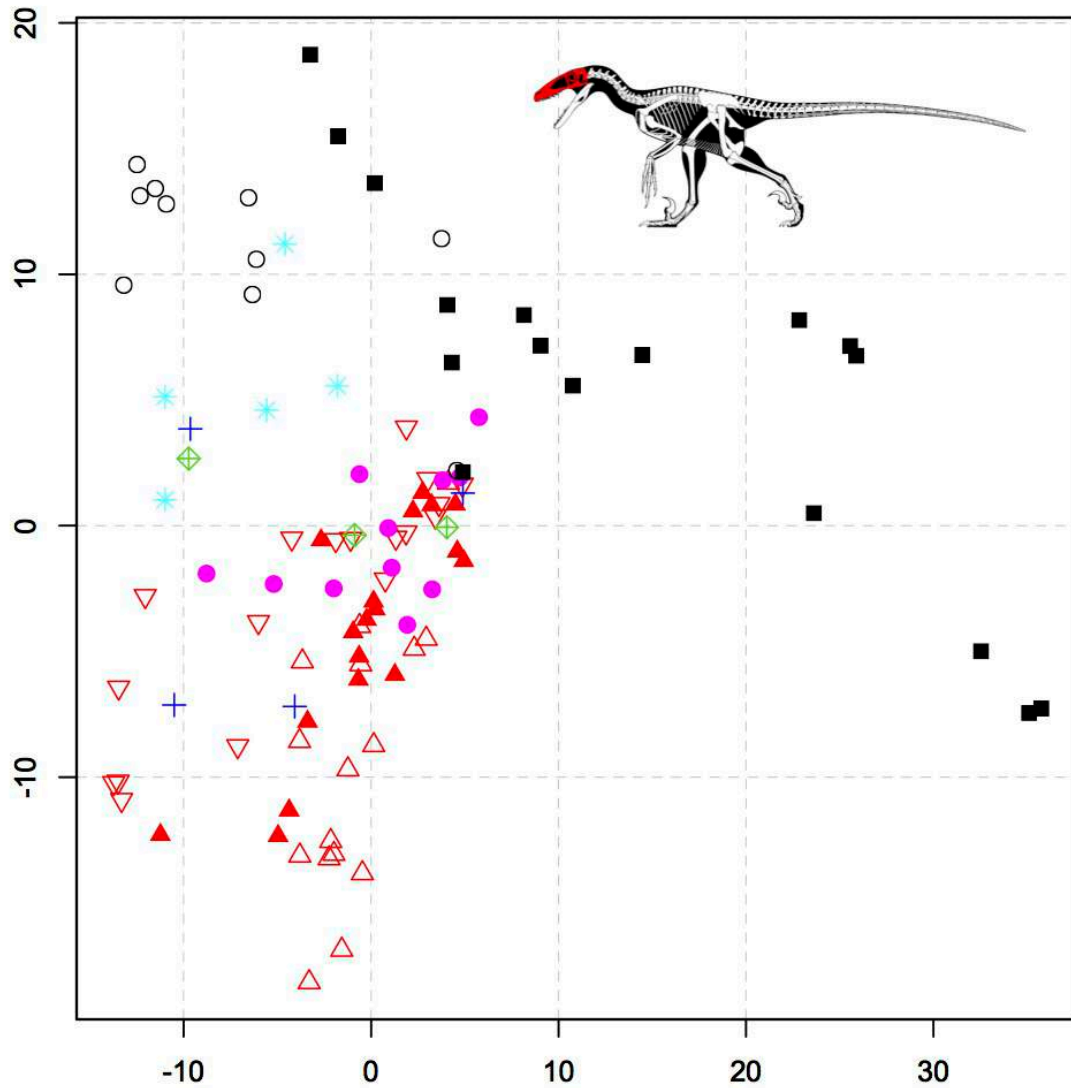


Figure 13. Facial disparity results based on taxa binned by clad. Disparity values based on the weighted mean pairwise disparity (WMPD) from the generalised Euclidean distance matrix (GED). 95% confidence intervals based on 10,000 bootstrap replicates are also plotted.

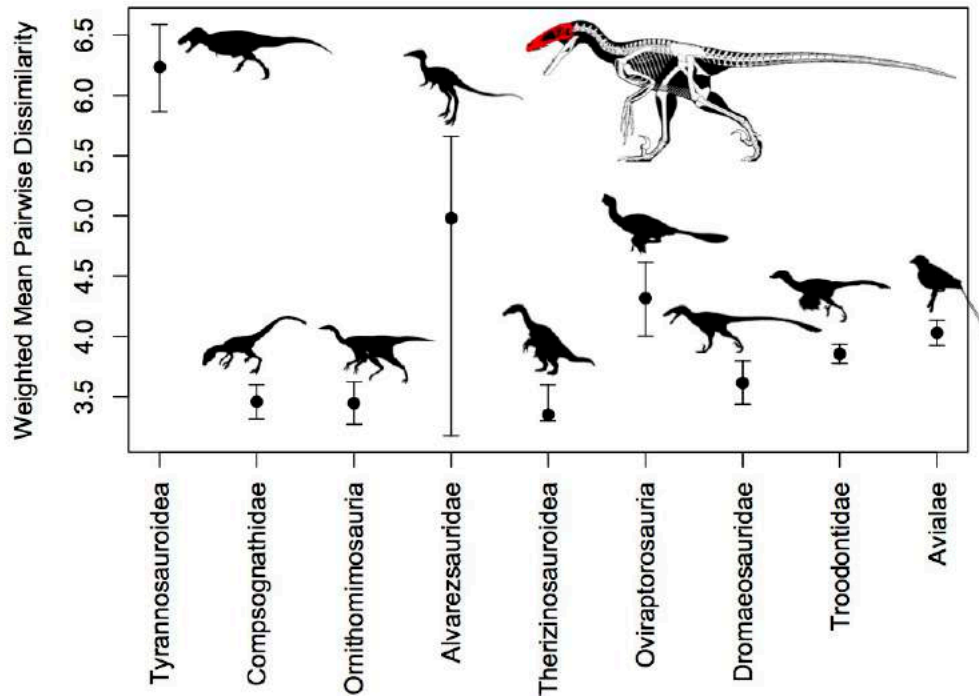


Figure 14. Facial disparity results based on taxa binned by clad. Disparity values based on the weighted mean pairwise disparity (WMPD) from the sum of variances from PCO scores. 95% confidence intervals based on 10,000 bootstrap replicates are also plotted.

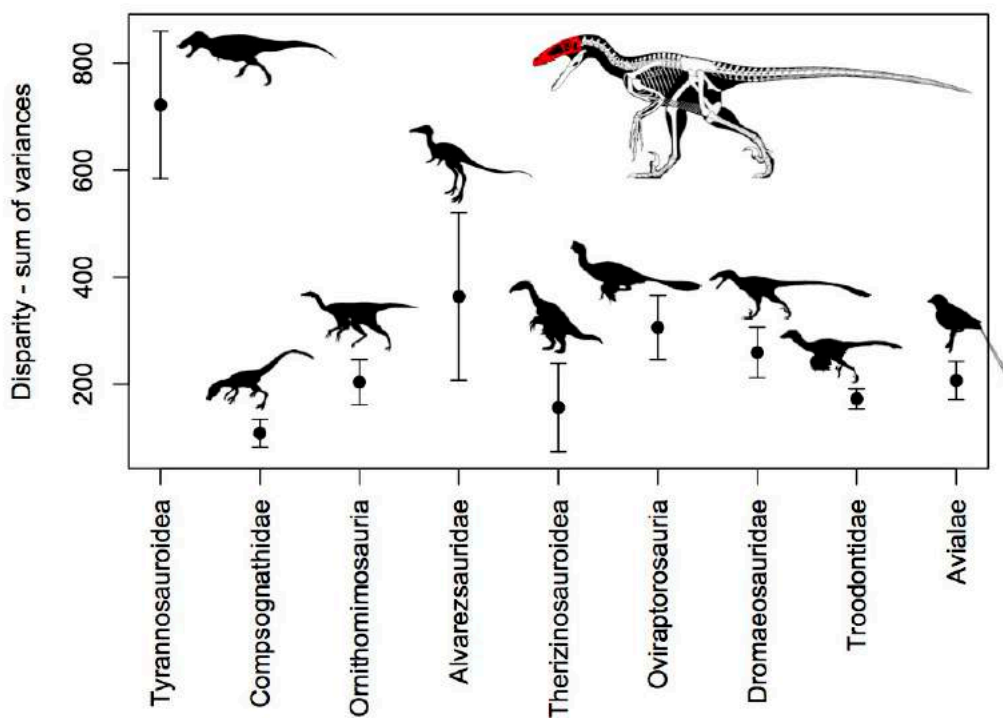


Figure 15. Temporal disparity trend of the facial skeleton in Coelurosauria.

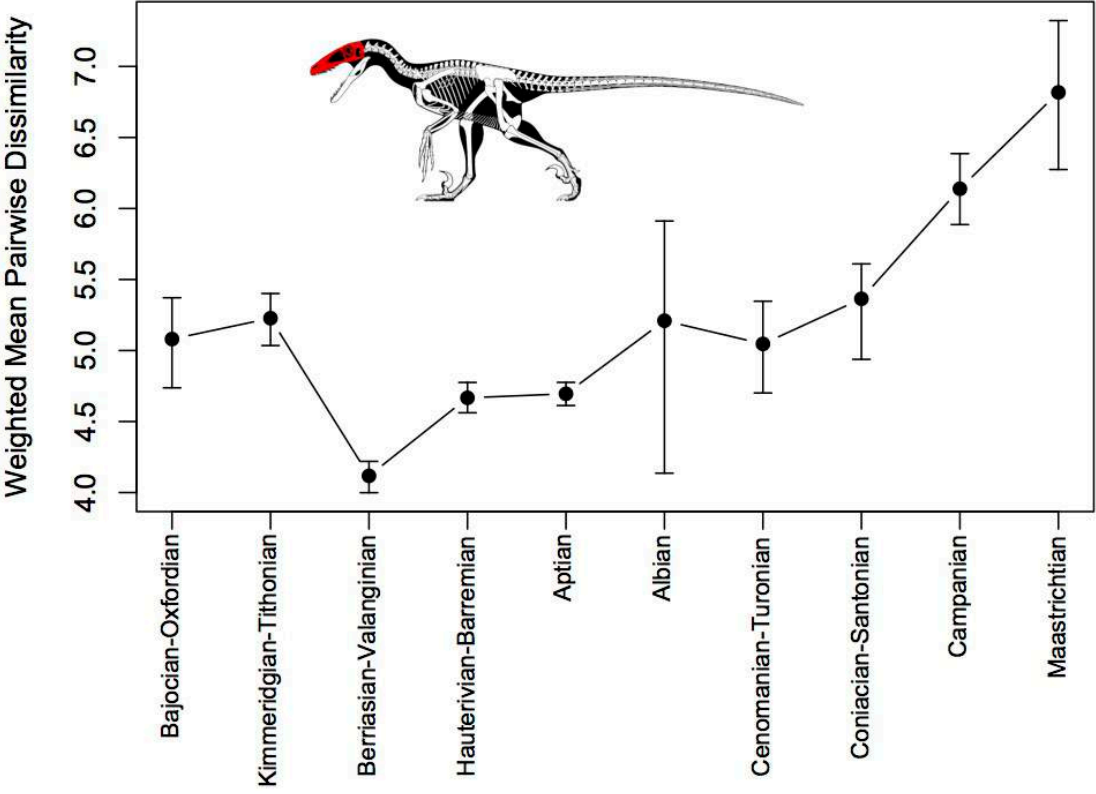


Figure 16. Rates of morphological evolution based on mandibular characters in coelurosaurian theropods. The proportion of significantly high (red) and significantly low (blue) per-branch rates based on 100 dating replications are illustrated with pie charts.

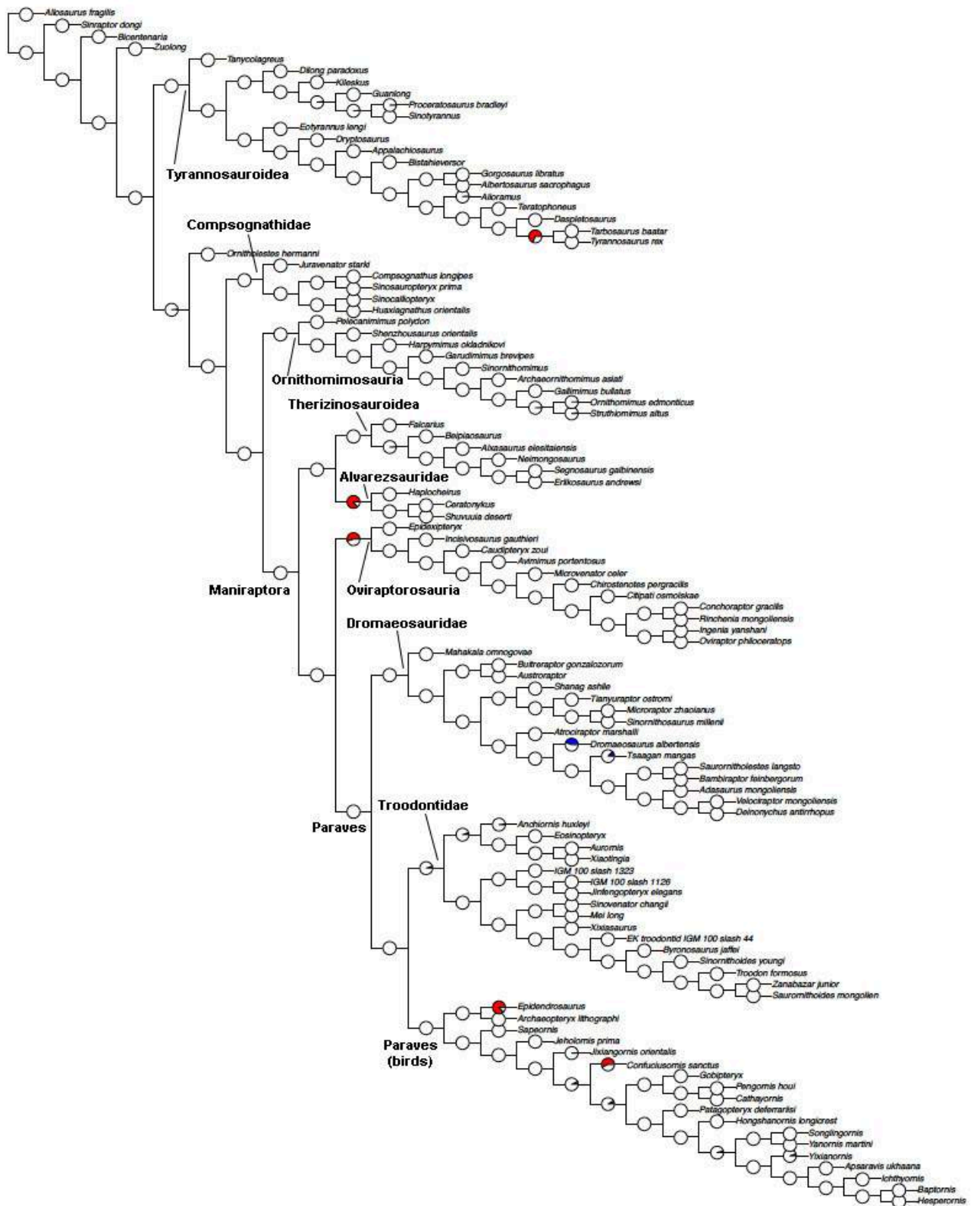


Figure 17. Disparity morphospace resulting from Principal Coordinate Analysis (PCO) for the mandible in various coelurosaurian clades. Black squares = Tyrannosauroidae; blue asterisks = Compsognathidae; empty circles = Ornithomimosauria; blue crosses = Alvarezsauridae; pink solid circles = Oviraptorosauria; green rhombs = Therizinosauria; empty red triangles pointing up = Dromaeosauridae; empty red triangles pointing down = Troodontidae; red solid triangles = Avialae (birds).

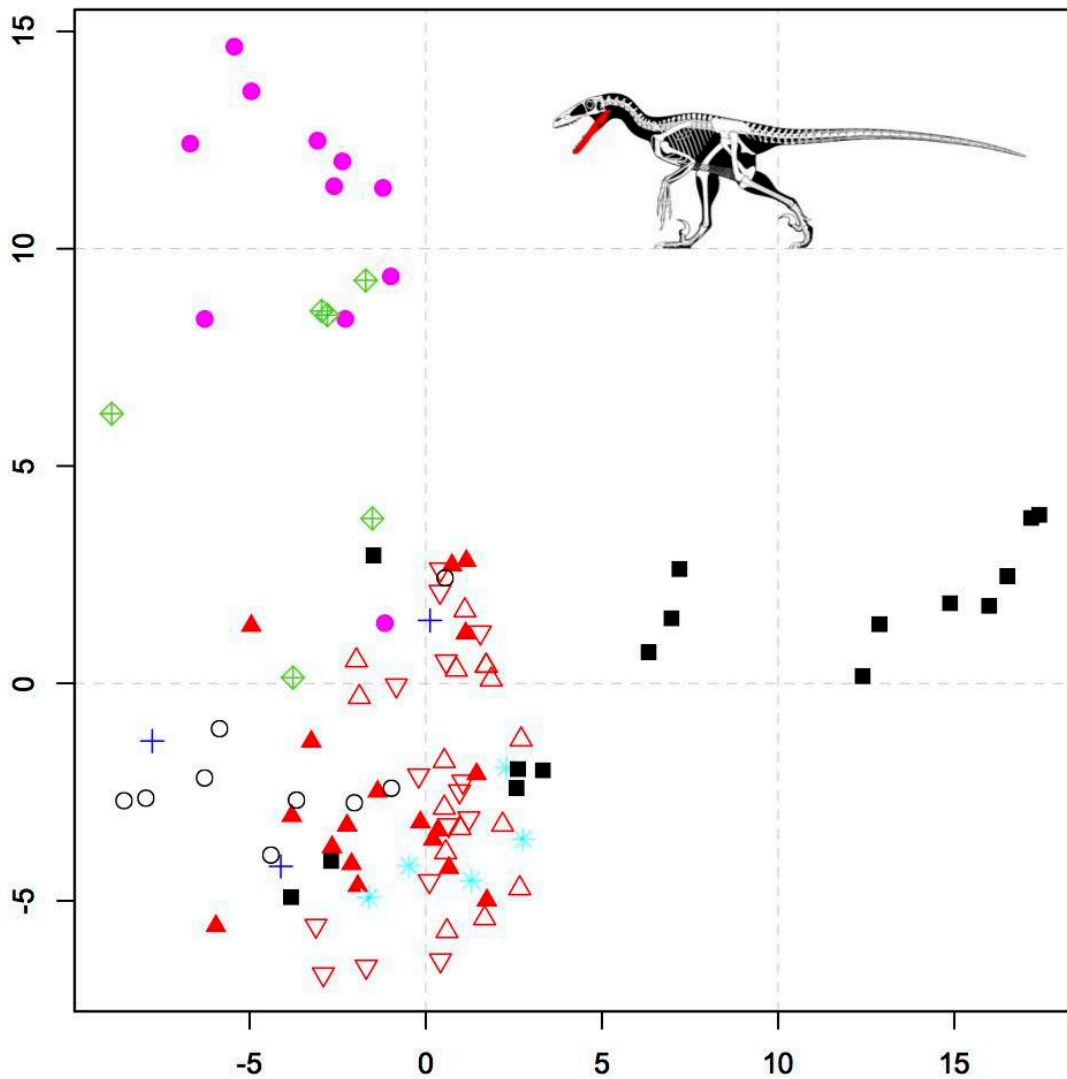


Figure 18. Mandibular disparity results based on taxa binned by clad. Disparity values based on the weighted mean pairwise disparity (WMPD) from the generalised Euclidean distance matrix (GED). 95% confidence intervals based on 10,000 bootstrap replicates are also plotted.

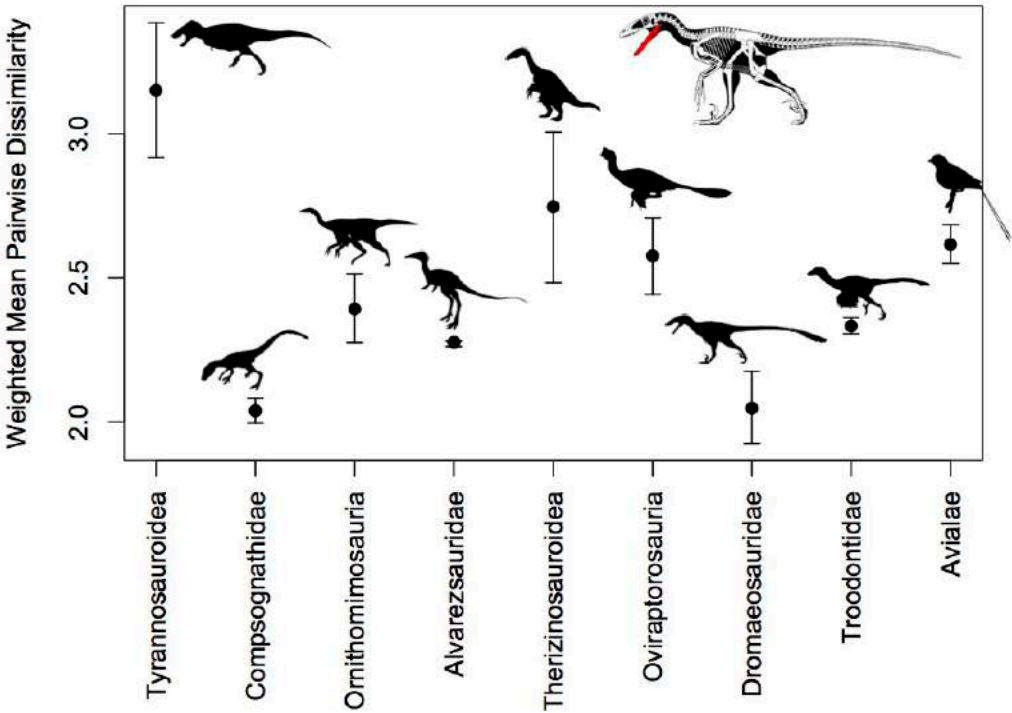


Figure 19. Mandibular disparity results based on taxa binned by clad. Disparity values based on the weighted mean pairwise disparity (WMPD) from the sum of variances from PCO scores. 95% confidence intervals based on 10,000 bootstrap replicates are also plotted.

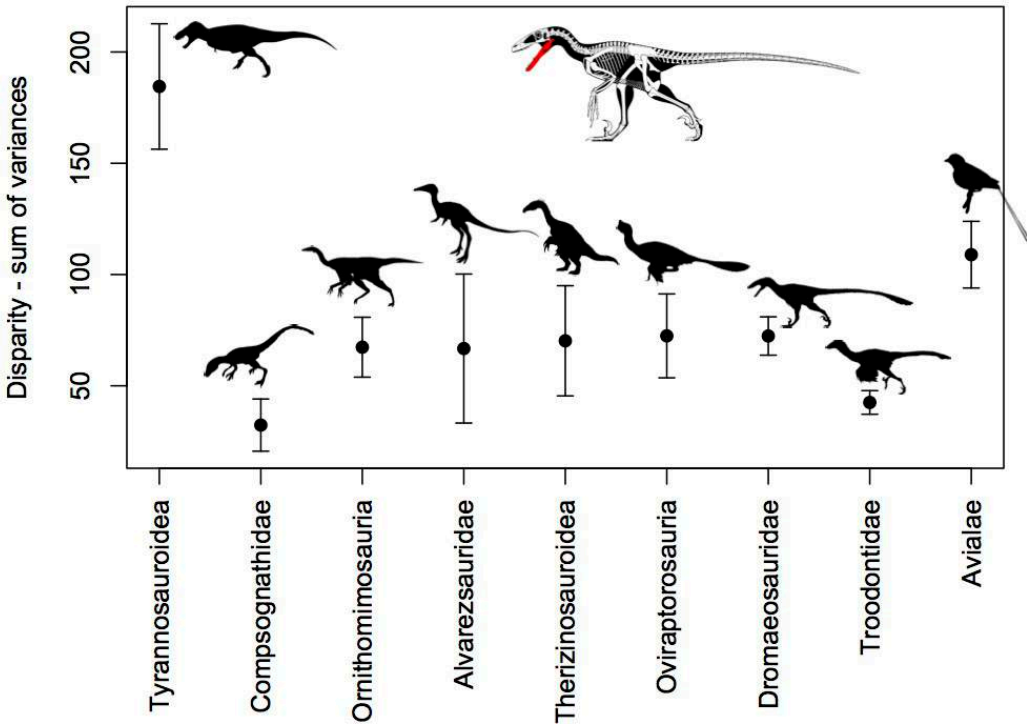


Figure 20. Temporal disparity trend of the mandible in coelurosaurian theropods.

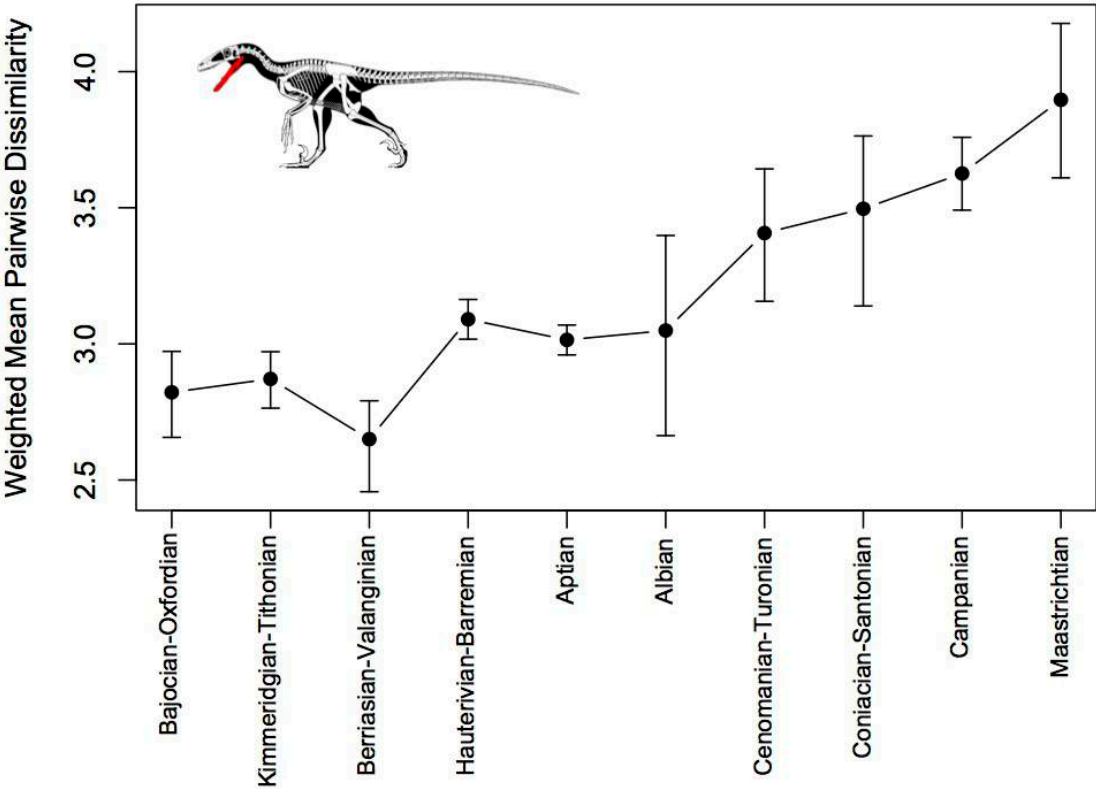


Figure 21. Rates of morphological evolution based on dental characters in Coelurosauria. The proportion of significantly high (red) and significantly low (blue) per-branch rates based on 100 dating replications are illustrated with pie charts.

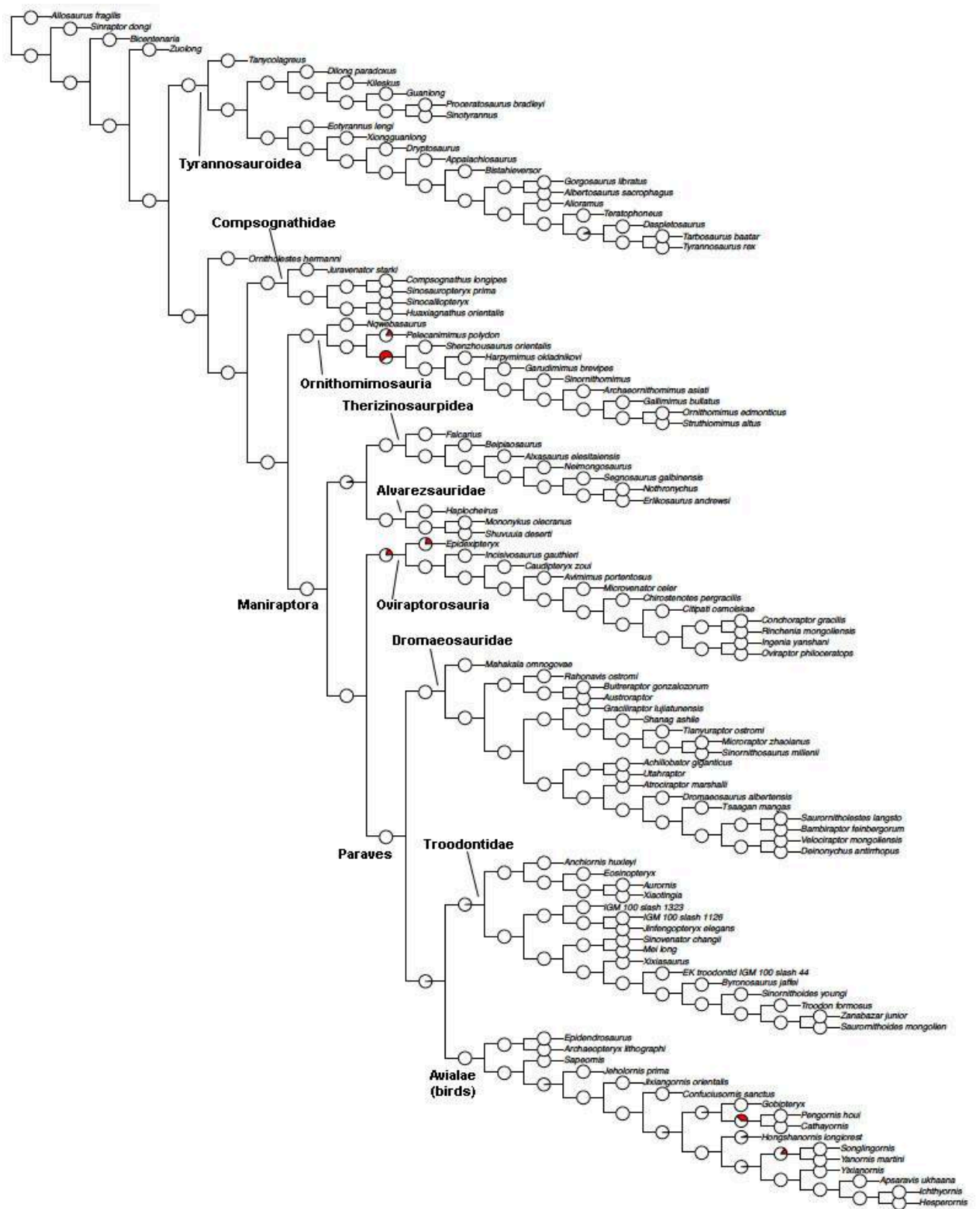


Figure 22. Disparity morphospace resulting from Principal Coordinate Analysis (PCO) for the dentition in various coelurosaurian clades. Black squares = Tyrannosauoidea; blue asterisks = Compsognathidae; empty circles = Ornithomimosauria; blue crosses = Alvarezsauridae; pink solid circles = Oviraptorosauria; green rhombs = Therizinosauria; empty red triangles pointing up = Dromaeosauridae; empty red triangles pointing down = Troodontidae; red solid triangles = Avialae (birds).

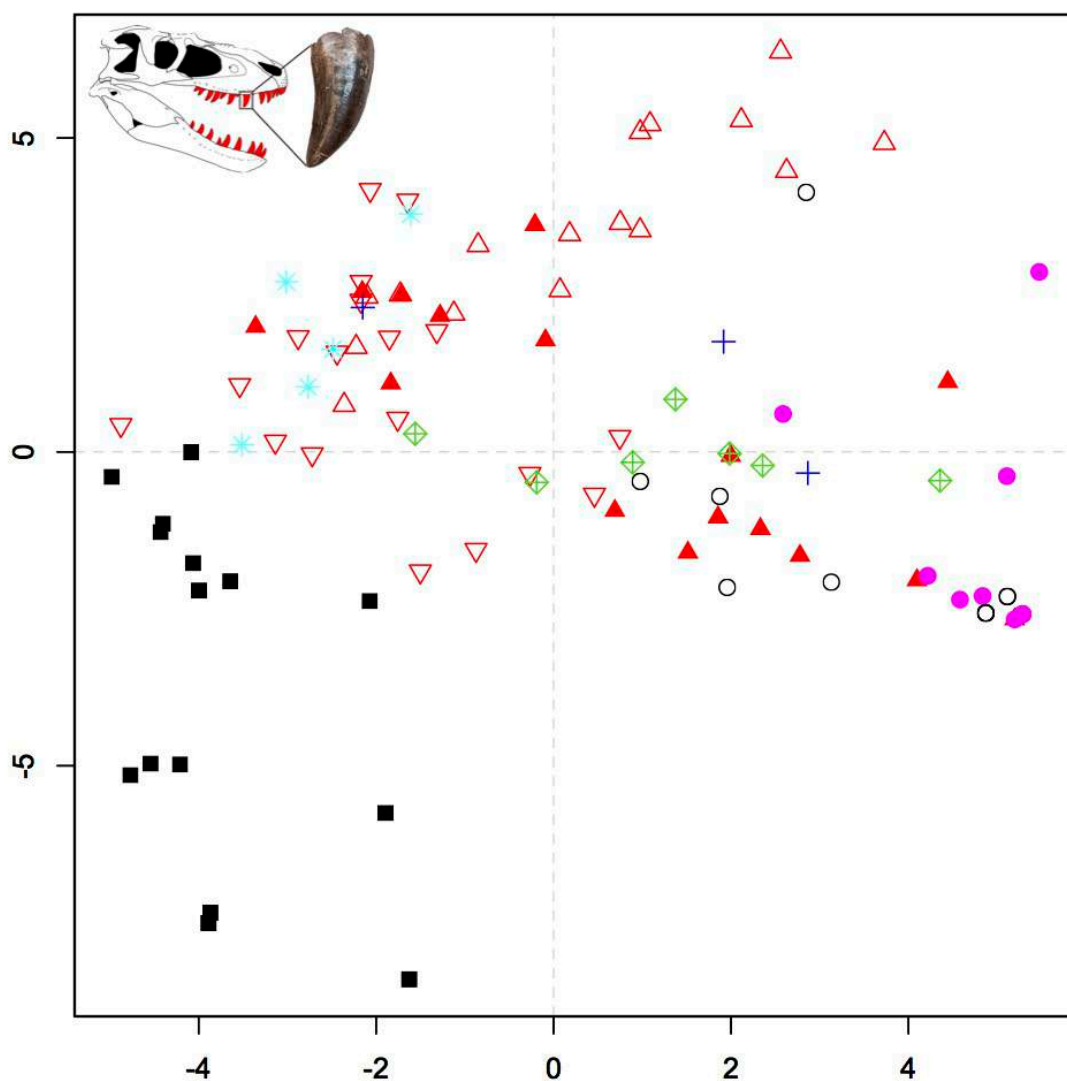


Figure 23. Dental disparity results based on taxa binned by clad. Disparity values based on the weighted mean pairwise disparity (WMPD) from the generalised Euclidean distance matrix (GED). 95% confidence intervals based on 10,000 bootstrap replicates are also plotted.

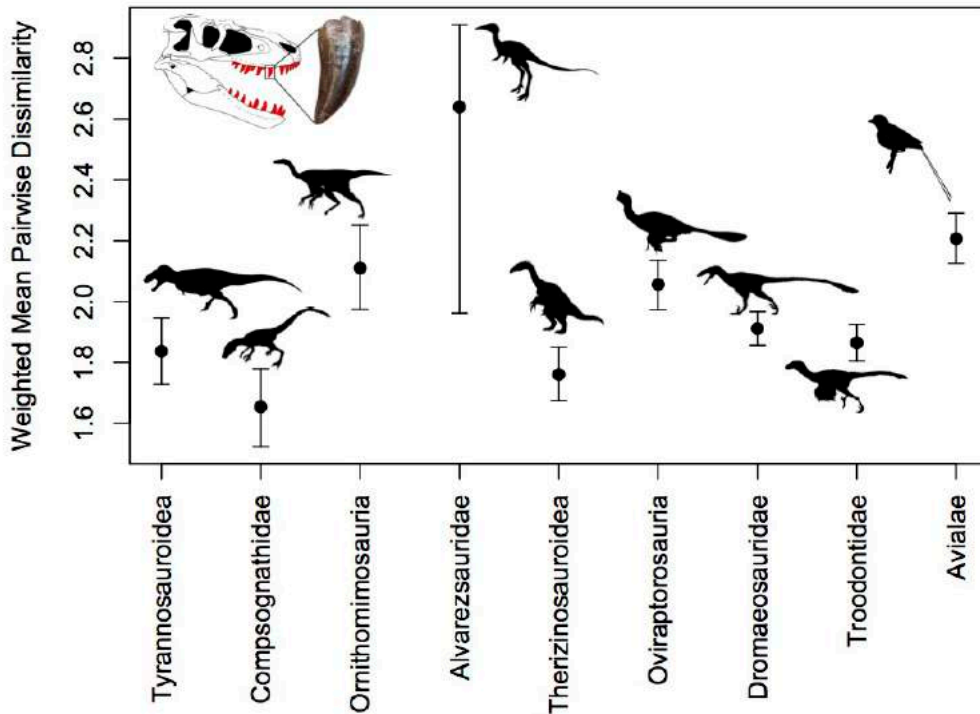


Figure 24. Dental disparity results based on taxa binned by clad. Disparity values based on the weighted mean pairwise disparity (WMPD) from the sum of variances from PCO scores. 95% confidence intervals based on 10,000 bootstrap replicates are also plotted.

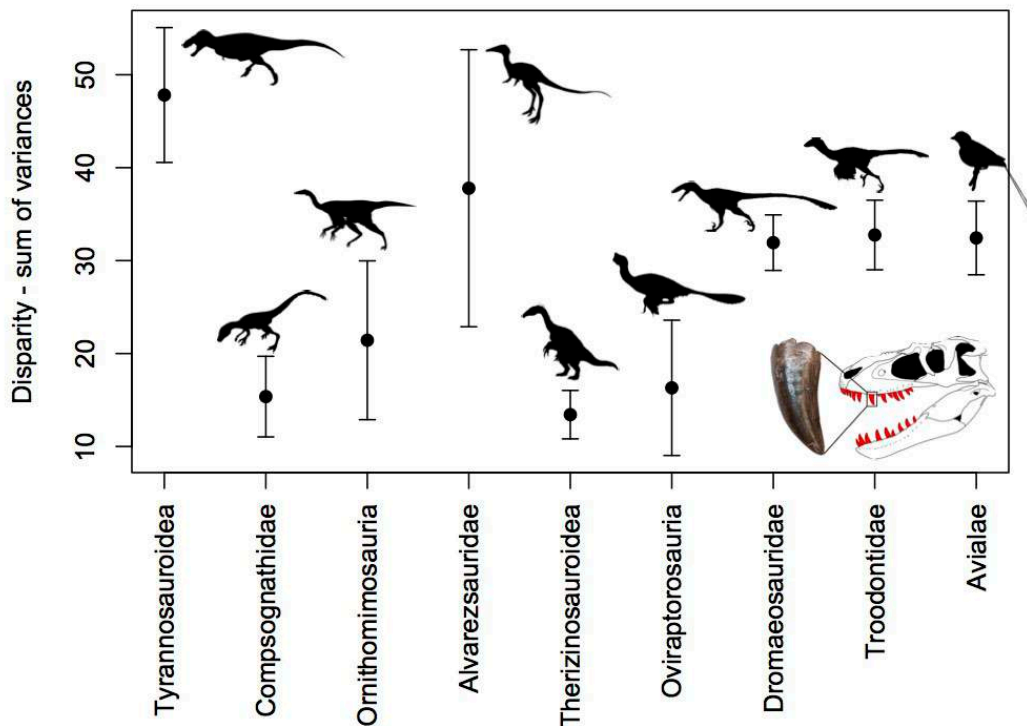


Figure 25. Temporal disparity trend of the dentition in coelurosaurian theropods.

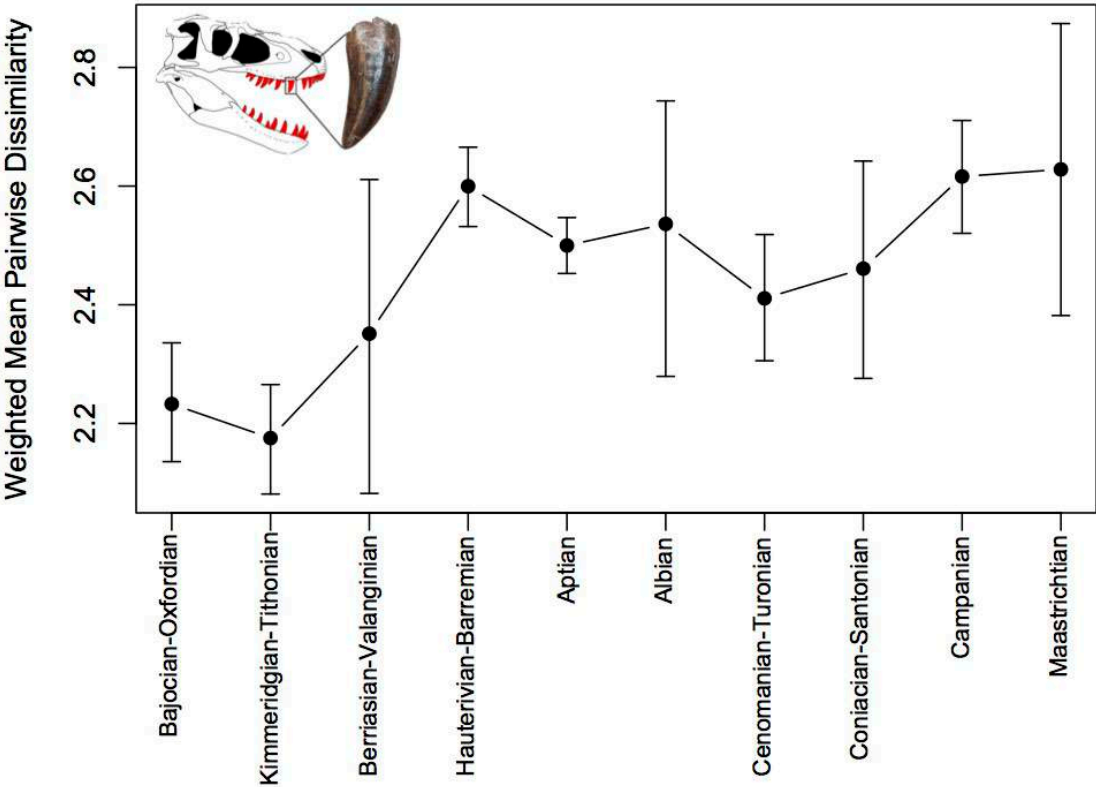


Figure 26. Rates of morphological evolution based on the entire postcranium characters in Coelurosauria. The proportion of significantly high (red) and significantly low (blue) per-branch rates based on 100 dating replications are illustrated with pie charts.

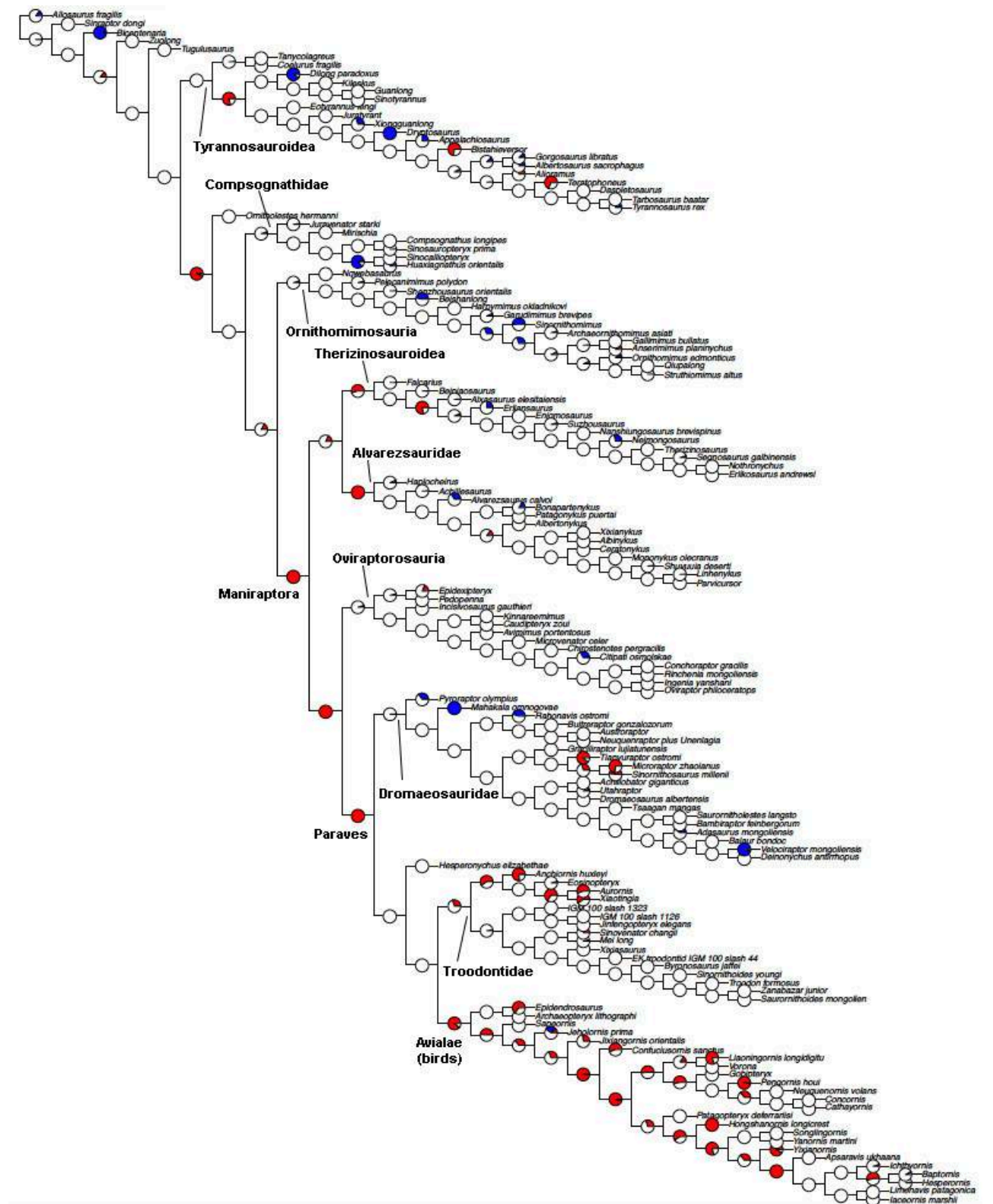


Figure 27. Disparity morphospace resulting from Principal Coordinate Analysis (PCO) for the entire postcranium in various coelurosaurian clades. Black squares = Tyrannosauroidae; blue asterisks = Compsognathidae; empty circles = Ornithomimosauria; blue crosses = Alvarezsauridae; pink solid circles = Oviraptorosauria; green rhombs = Therizinosauria; empty red triangles pointing up = Dromaeosauridae; empty red triangles pointing down = Troodontidae; red solid triangles = Avialae (birds).

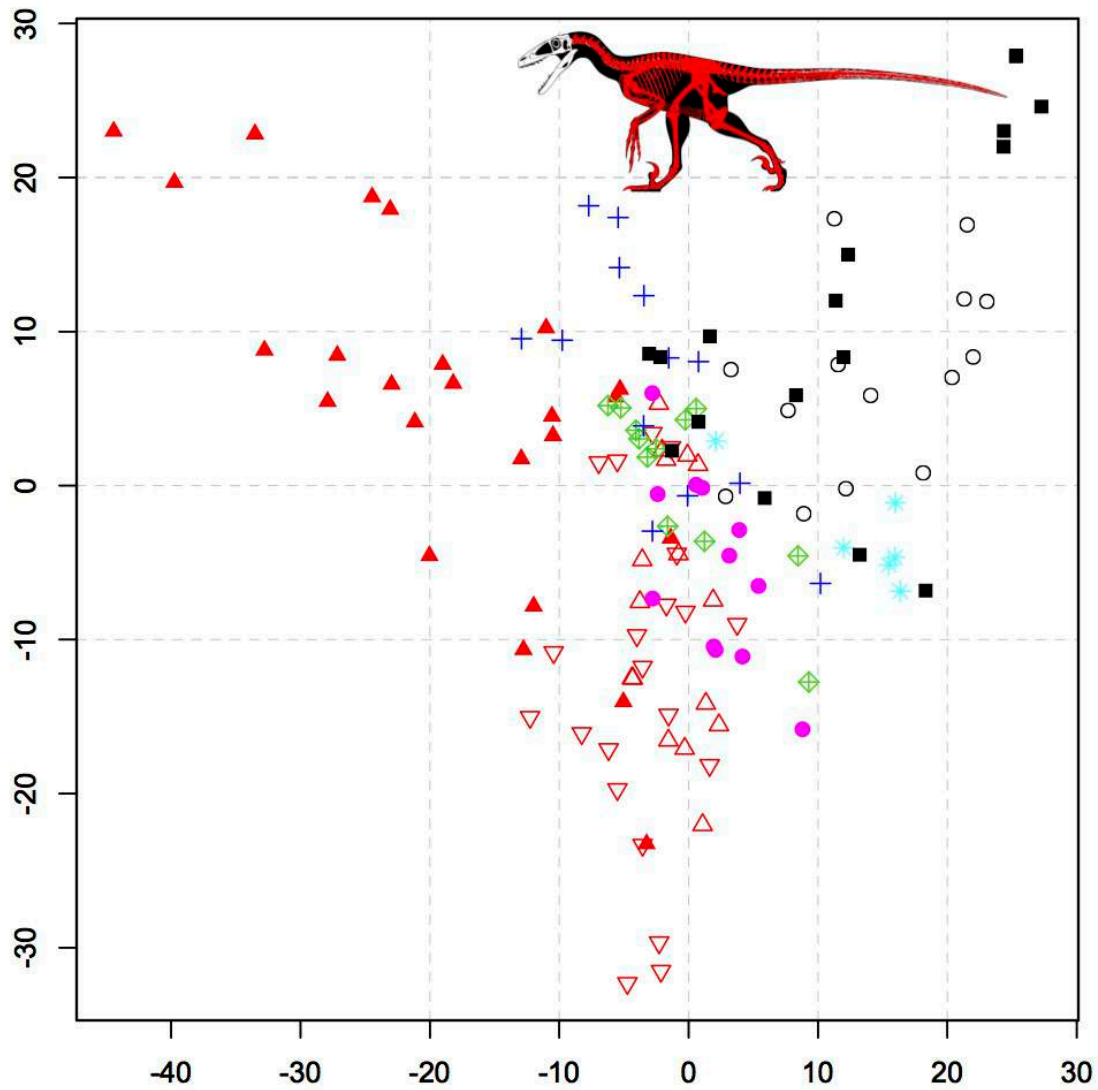


Figure 28. Postcranial disparity results based on taxa binned by clade. Disparity values based on the weighted mean pairwise disparity (WMPD) from the generalised Euclidean distance matrix (GED). 95% confidence intervals based on 10,000 bootstrap replicates are also plotted.

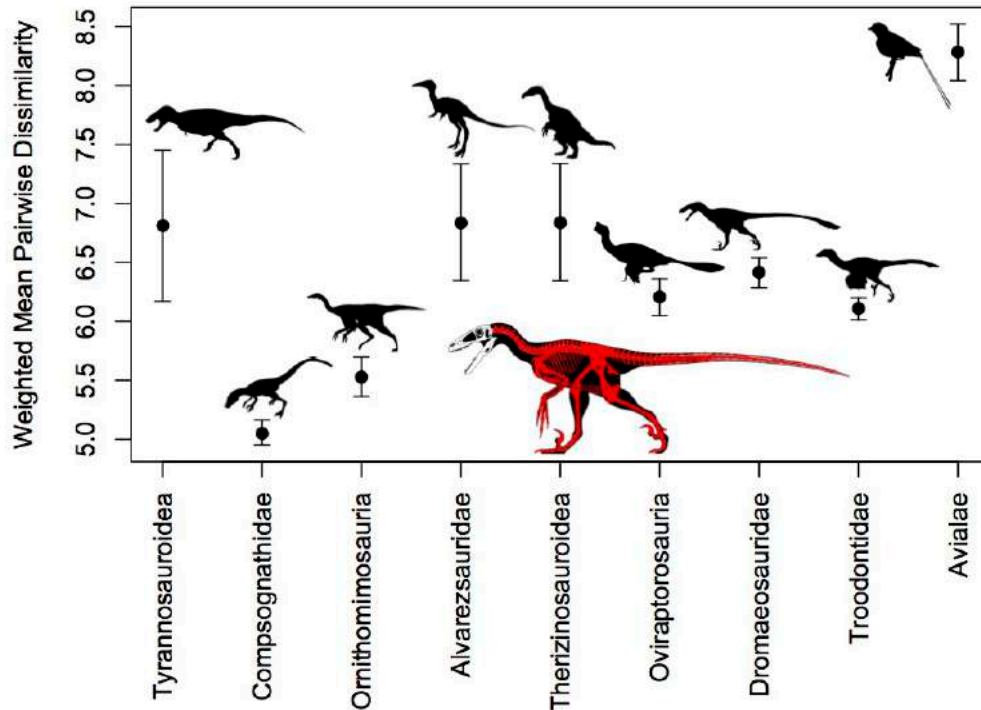


Figure 29. Postcranial disparity results based on taxa binned by clade. Disparity values based on the weighted mean pairwise disparity (WMPD) from the sum of variances from PCO scores. 95% confidence intervals based on 10,000 bootstrap replicates are also plotted.

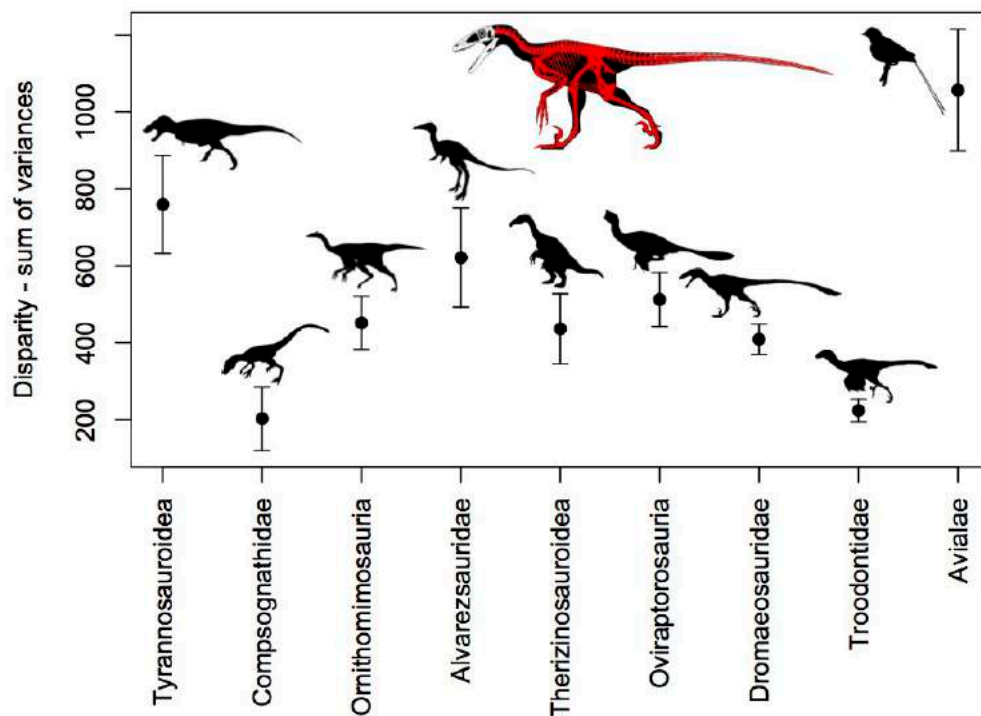


Figure 30. Temporal disparity trend of the entire portcranium in Coelurosauria.

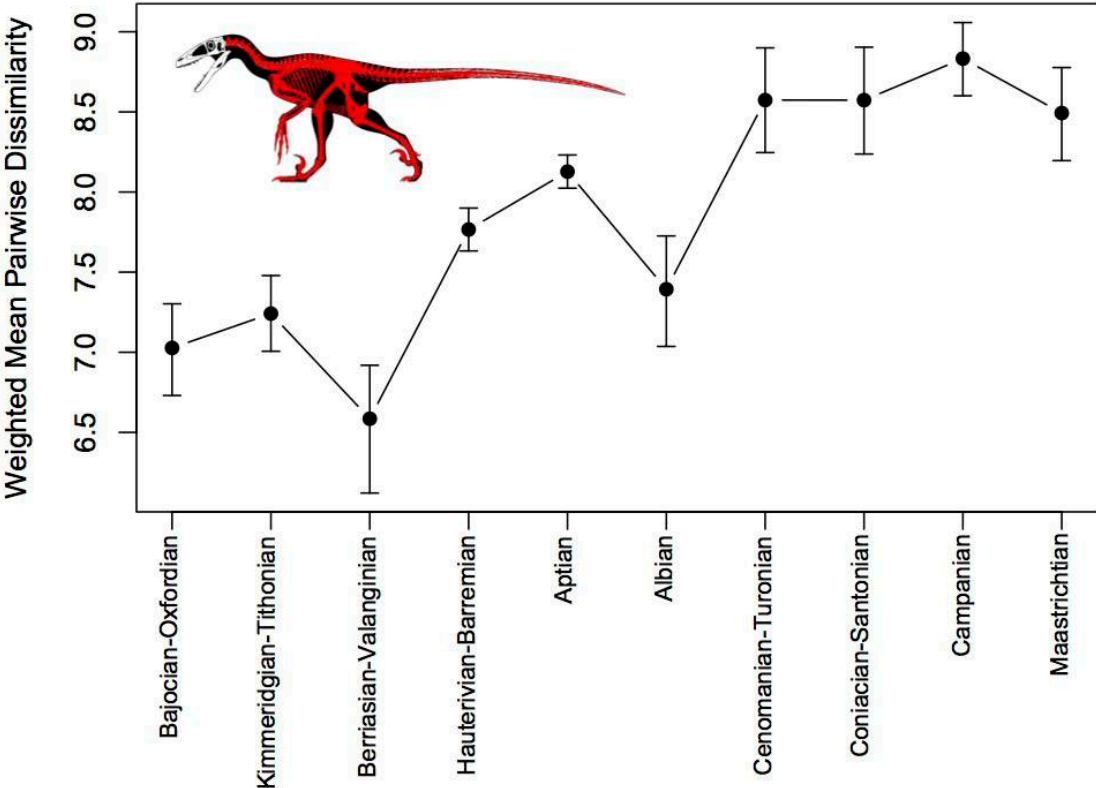


Figure 31. Rates of morphological evolution based on axial characters in Coelurosauria. The proportion of significantly high (red) and significantly low (blue) per-branch rates based on 100 dating replications are illustrated with pie charts.

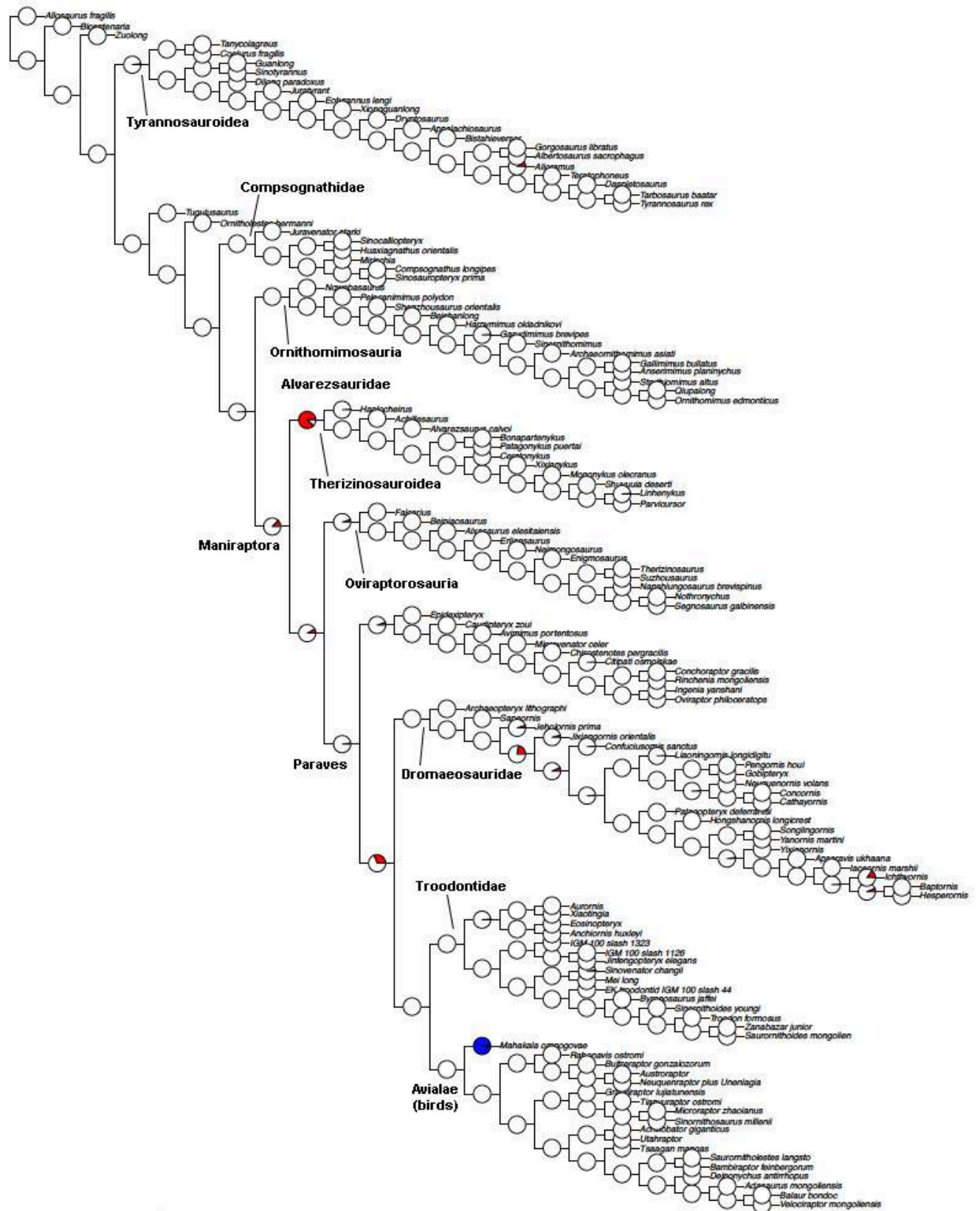


Figure 32. Disparity morphospace resulting from Principal Coordinate Analysis (PCO) for the axial skeleton in various coelurosaurian clades. Black squares = Tyrannosauroidae; blue asterisks = Compsognathidae; empty circles = Ornithomimosauria; blue crosses = Alvarezsauridae; pink solid circles = Oviraptorosauria; green rhombs = Therizinosauria; empty red triangles pointing up = Dromaeosauridae; empty red triangles pointing down = Troodontidae; red solid triangles = Avialae (birds).

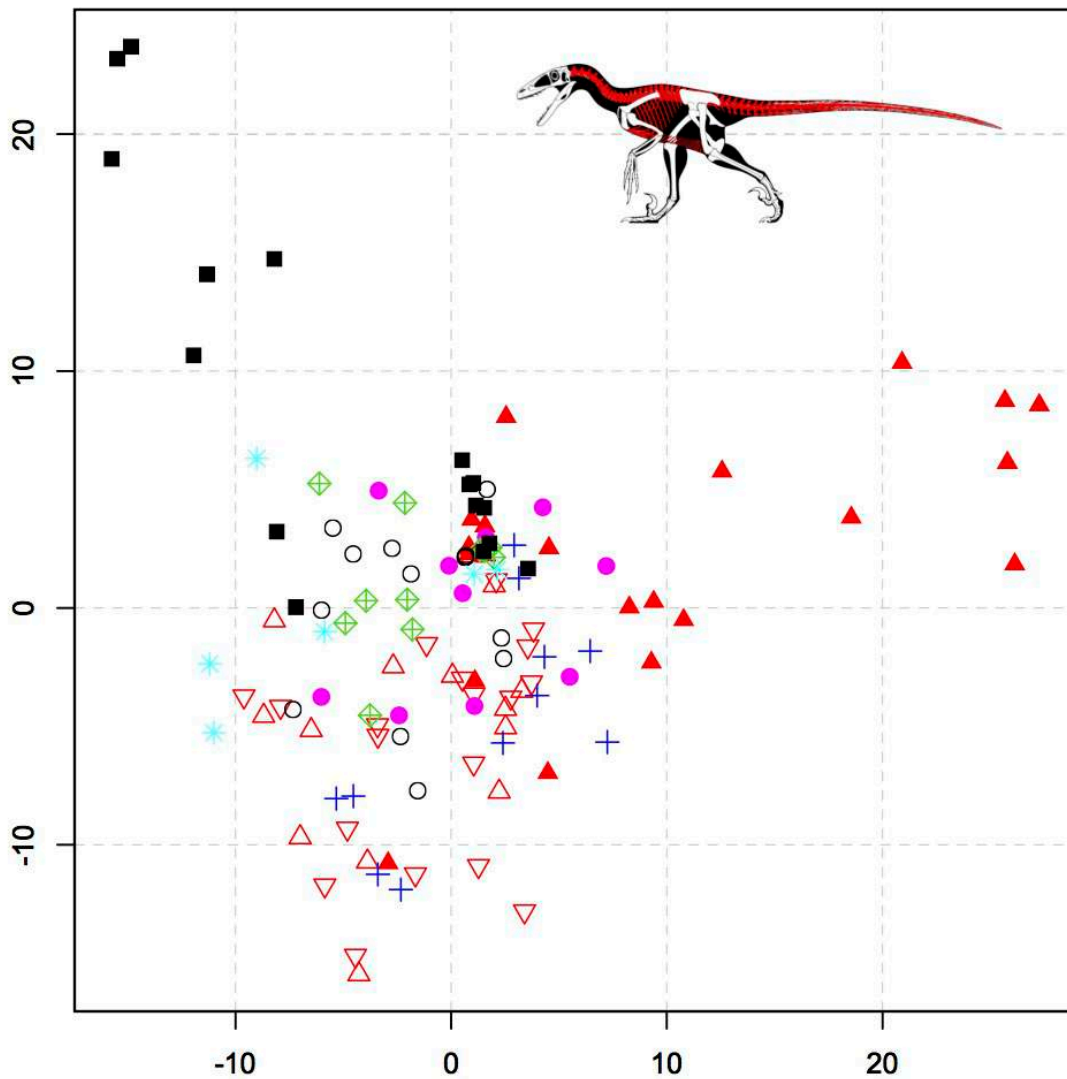


Figure 33. Axial disparity results based on taxa binned by clade. Disparity values based on the weighted mean pairwise disparity (WMPD) from the generalised Euclidean distance matrix (GED). 95% confidence intervals based on 10,000 bootstrap replicates are also plotted.

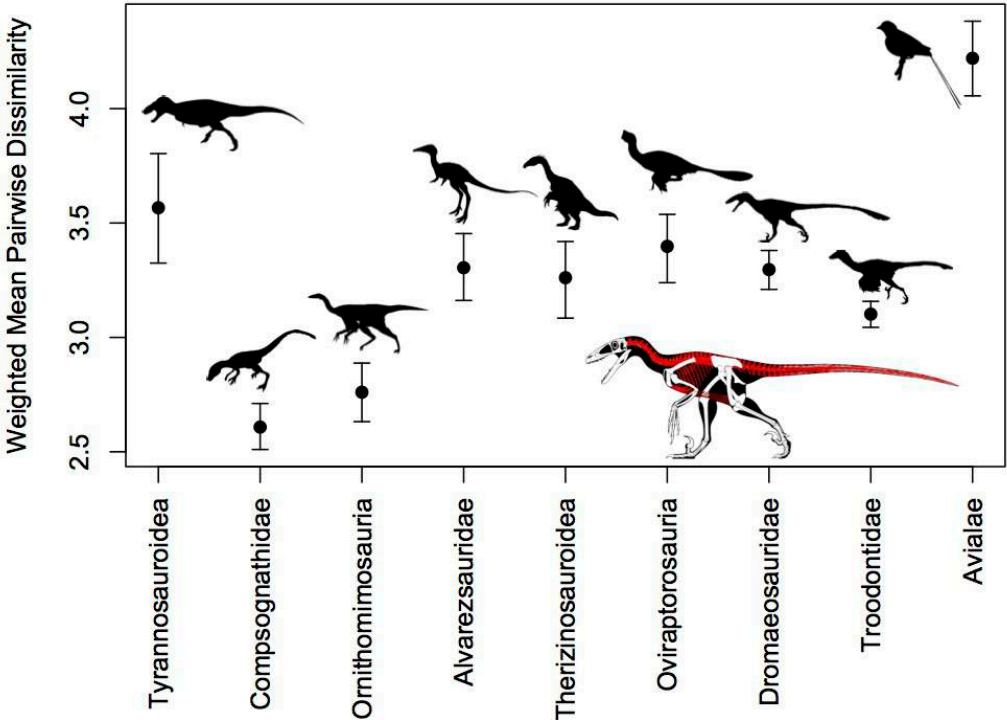


Figure 34. Axial disparity results based on taxa binned by clade. Disparity values based on the weighted mean pairwise disparity (WMPD) from the sum of variances from PCO scores. 95% confidence intervals based on 10,000 bootstrap replicates are also plotted.

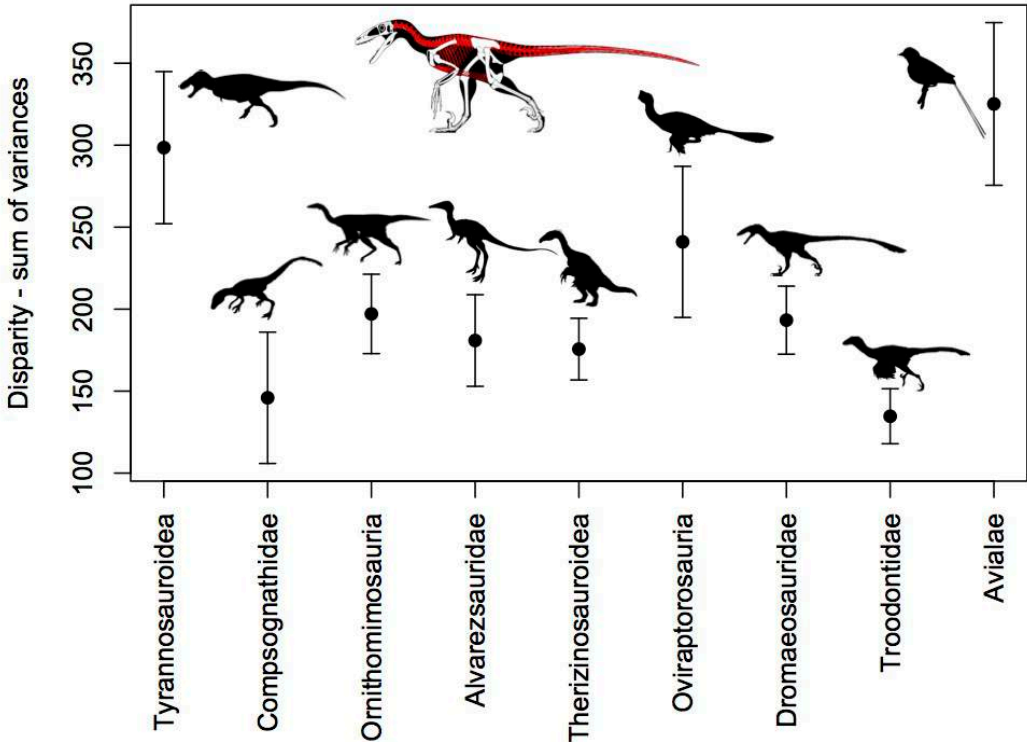


Figure 35. Temporal disparity trend of the axial skeleton in coelurosaurian theropods.

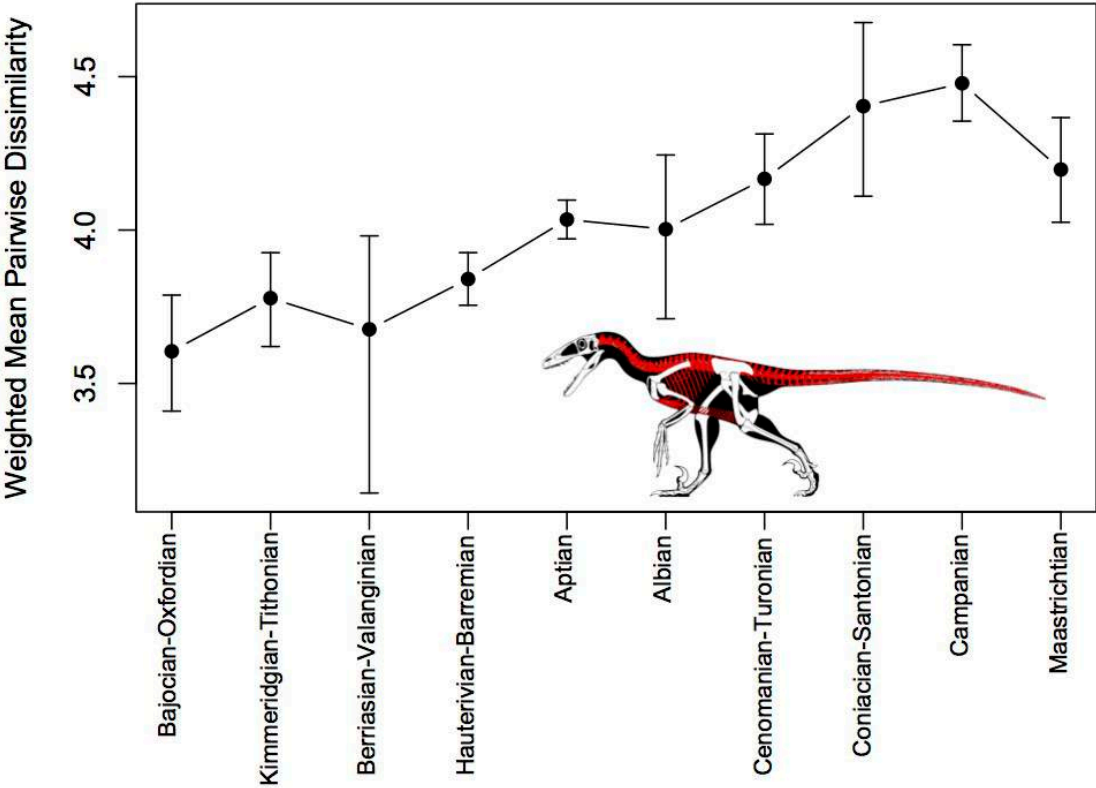


Figure 36. Rates of morphological evolution based on pectoral girdle characters in Coelurosauria. The proportion of significantly high (red) and significantly low (blue) per-branch rates based on 100 dating replications are illustrated with pie charts.

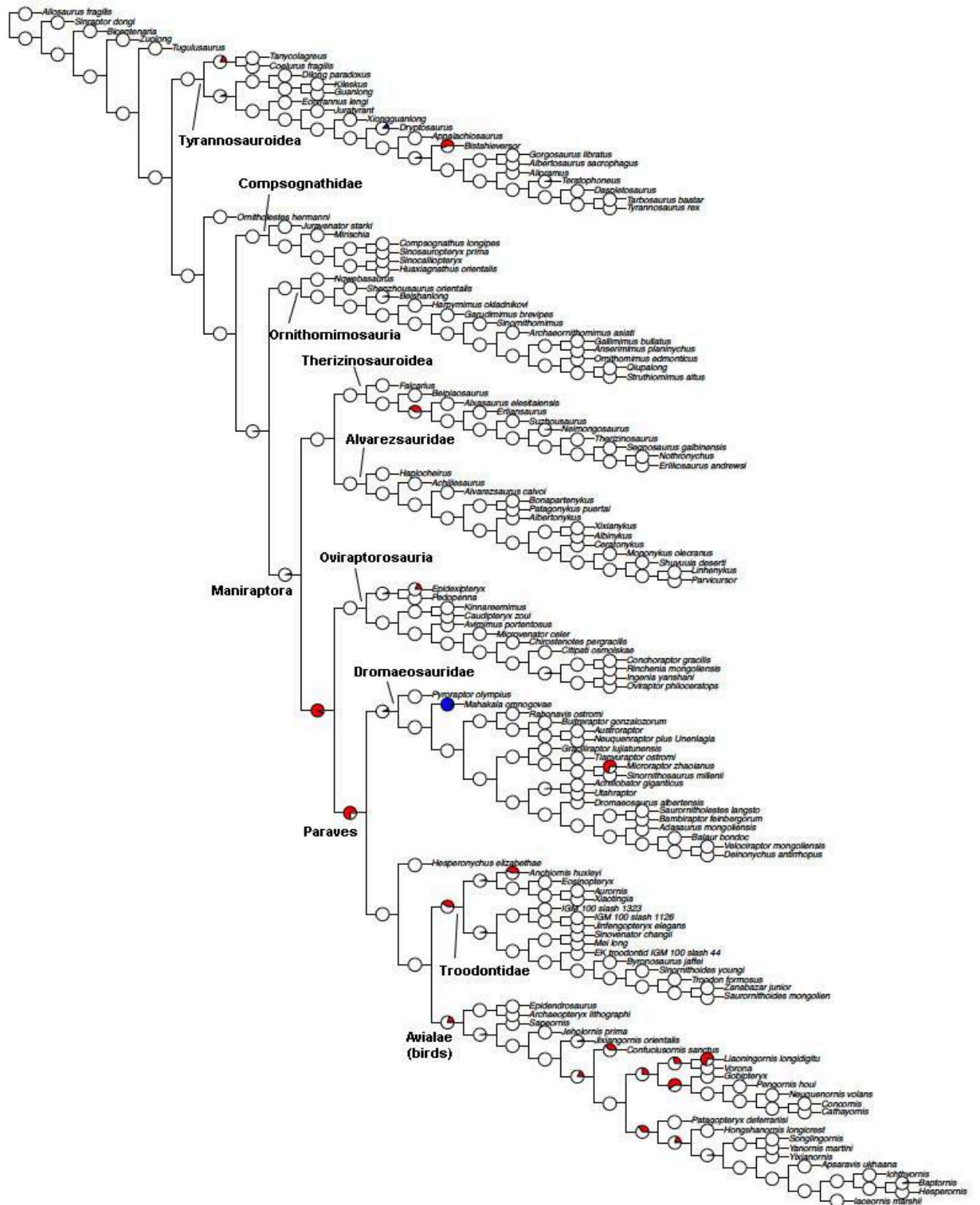


Figure 37. Disparity morphospace resulting from Principal Coordinate Analysis (PCO) for the pectoral girdle in various coelurosaurian clades. Black squares = Tyrannosauroidae; blue asterisks = Compsognathidae; empty circles = Ornithomimosauria; blue crosses = Alvarezsauridae; pink solid circles = Oviraptorosauria; green rhombs = Therizinosauria; empty red triangles pointing up = Dromaeosauridae; empty red triangles pointing down = Troodontidae; red solid triangles = Avialae (birds).

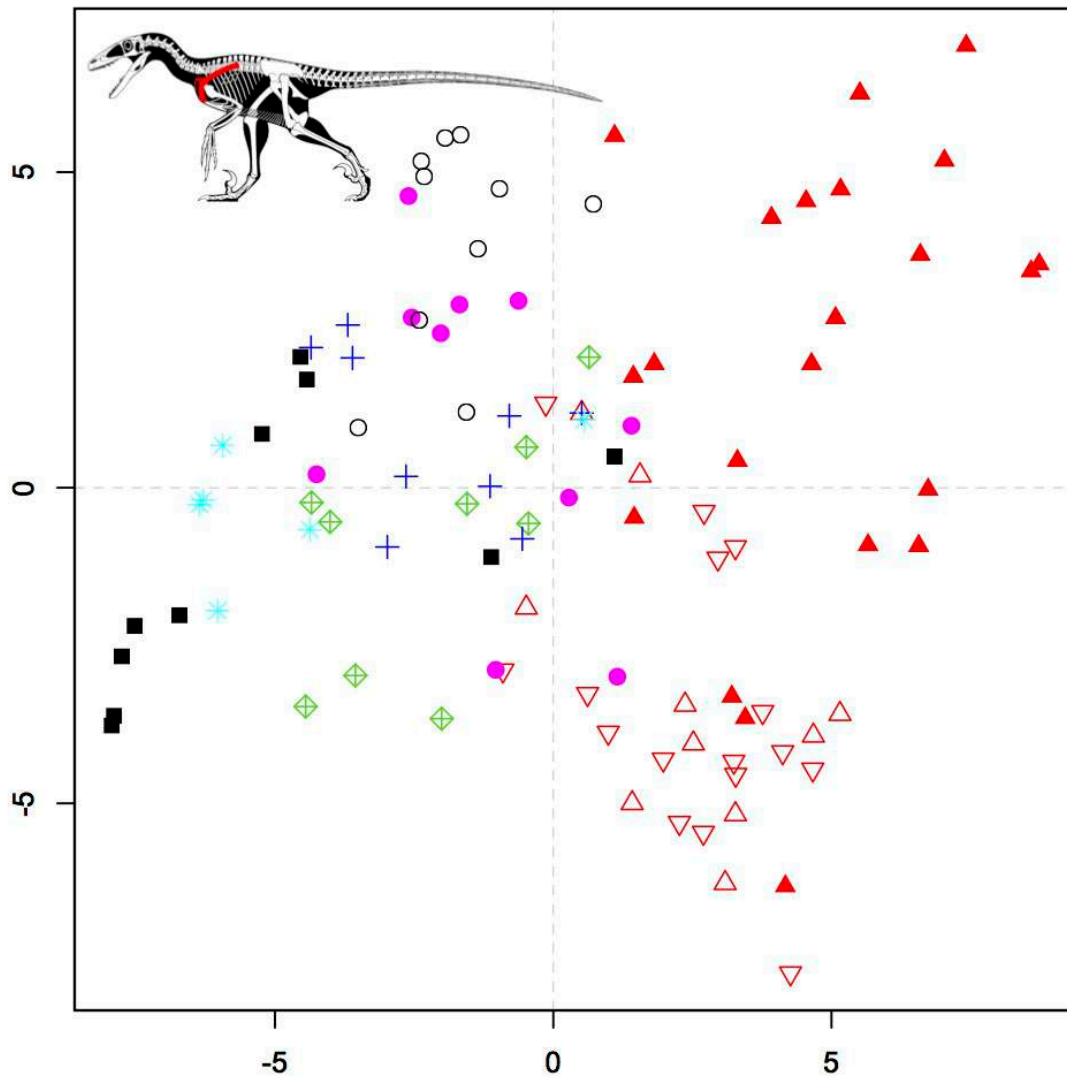


Figure 38. Pectoral disparity results based on taxa binned by clade. Disparity values based on the weighted mean pairwise disparity (WMPD) from the generalised Euclidean distance matrix (GED). 95% confidence intervals based on 10,000 bootstrap replicates are also plotted.

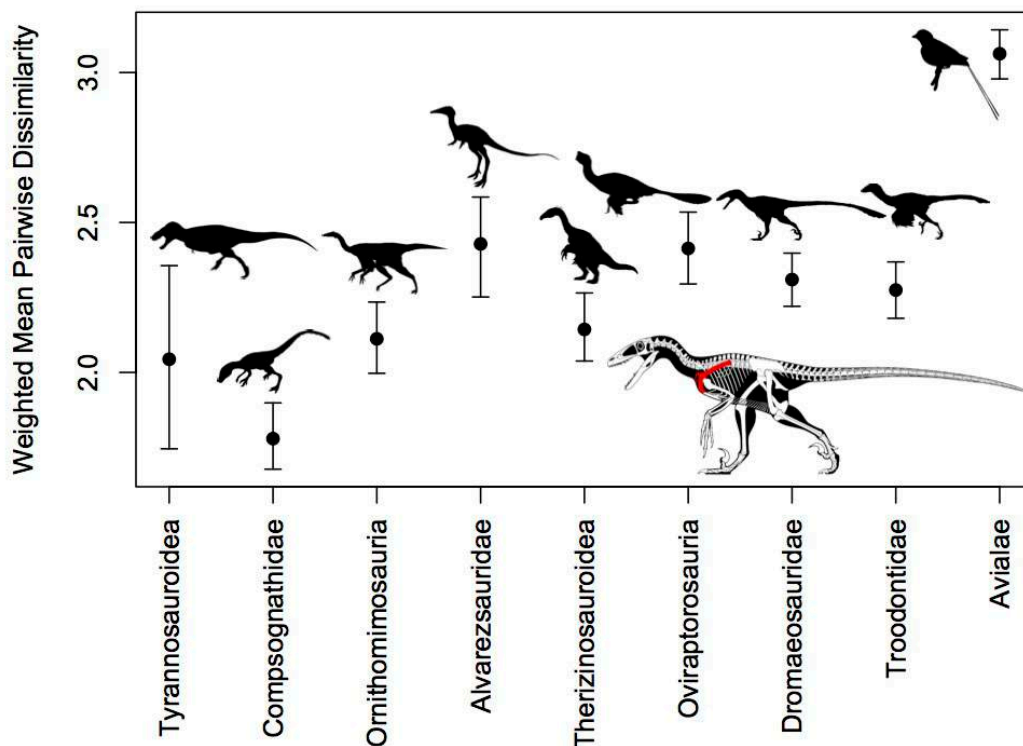


Figure 39. Pectoral disparity results based on taxa binned by clade. Disparity values based on the weighted mean pairwise disparity (WMPD) from the sum of variances from PCO scores. 95% confidence intervals based on 10,000 bootstrap replicates are also plotted.

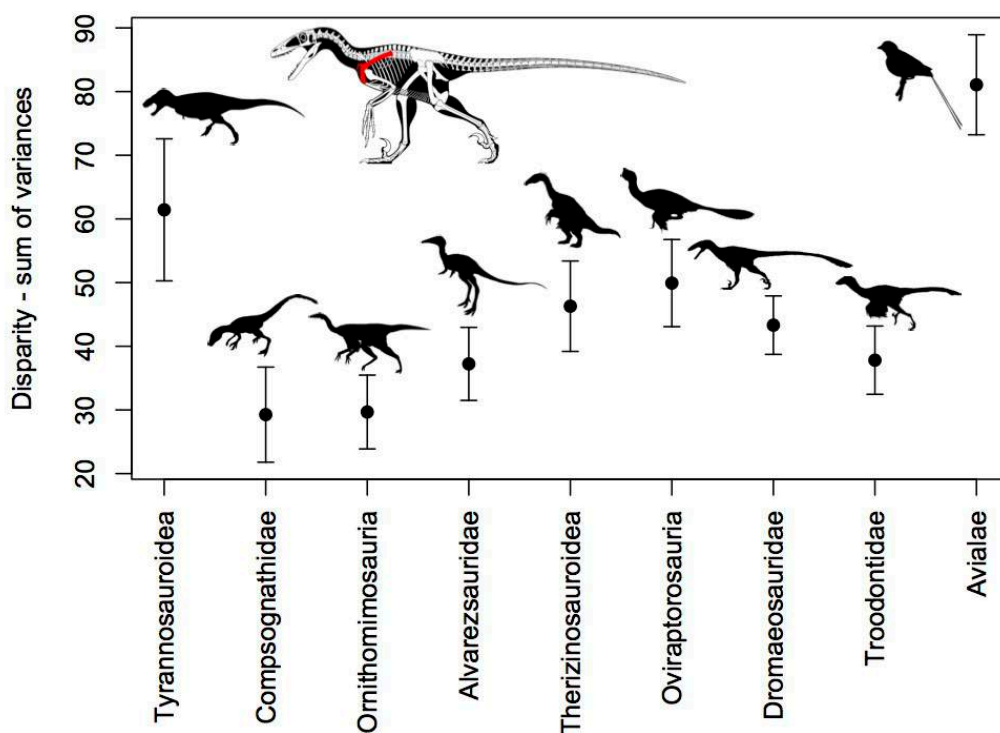


Figure 40. Temporal disparity trend of the pectoral girdle in Coelurosauria.

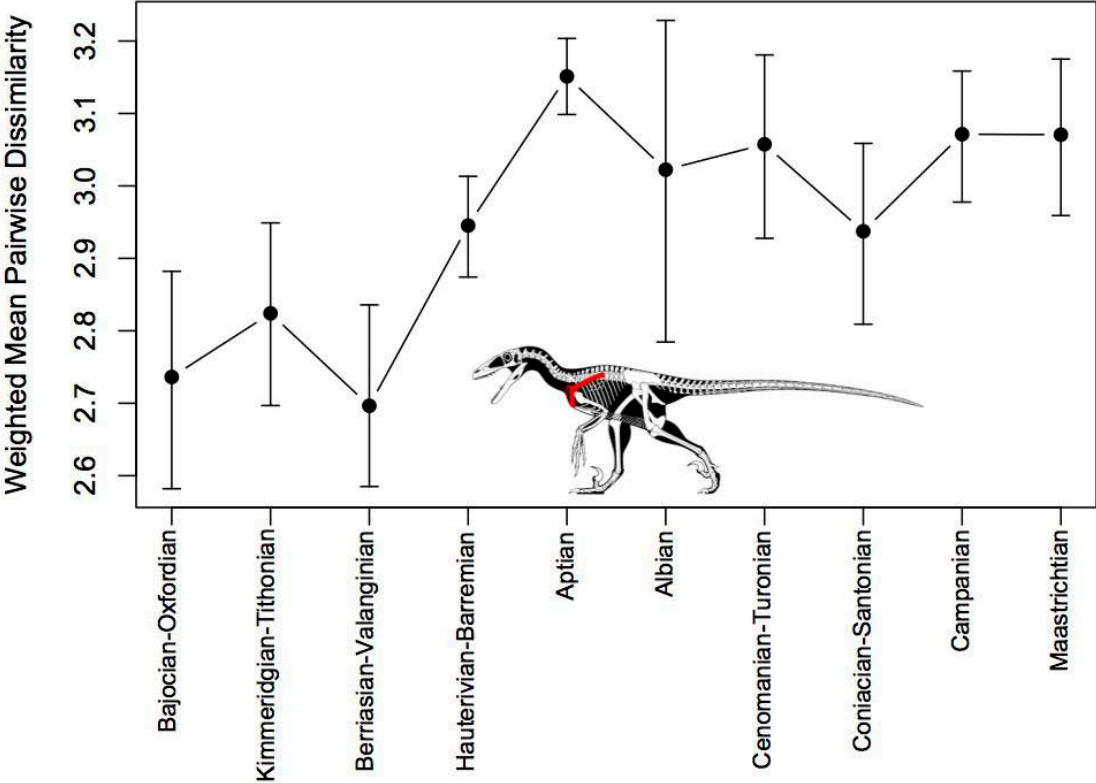


Figure 41. Rates of morphological evolution based on the forelimb in coelurosaurian theropods. The proportion of significantly high (red) and significantly low (blue) per-branch rates based on 100 dating replications are illustrated with pie charts.

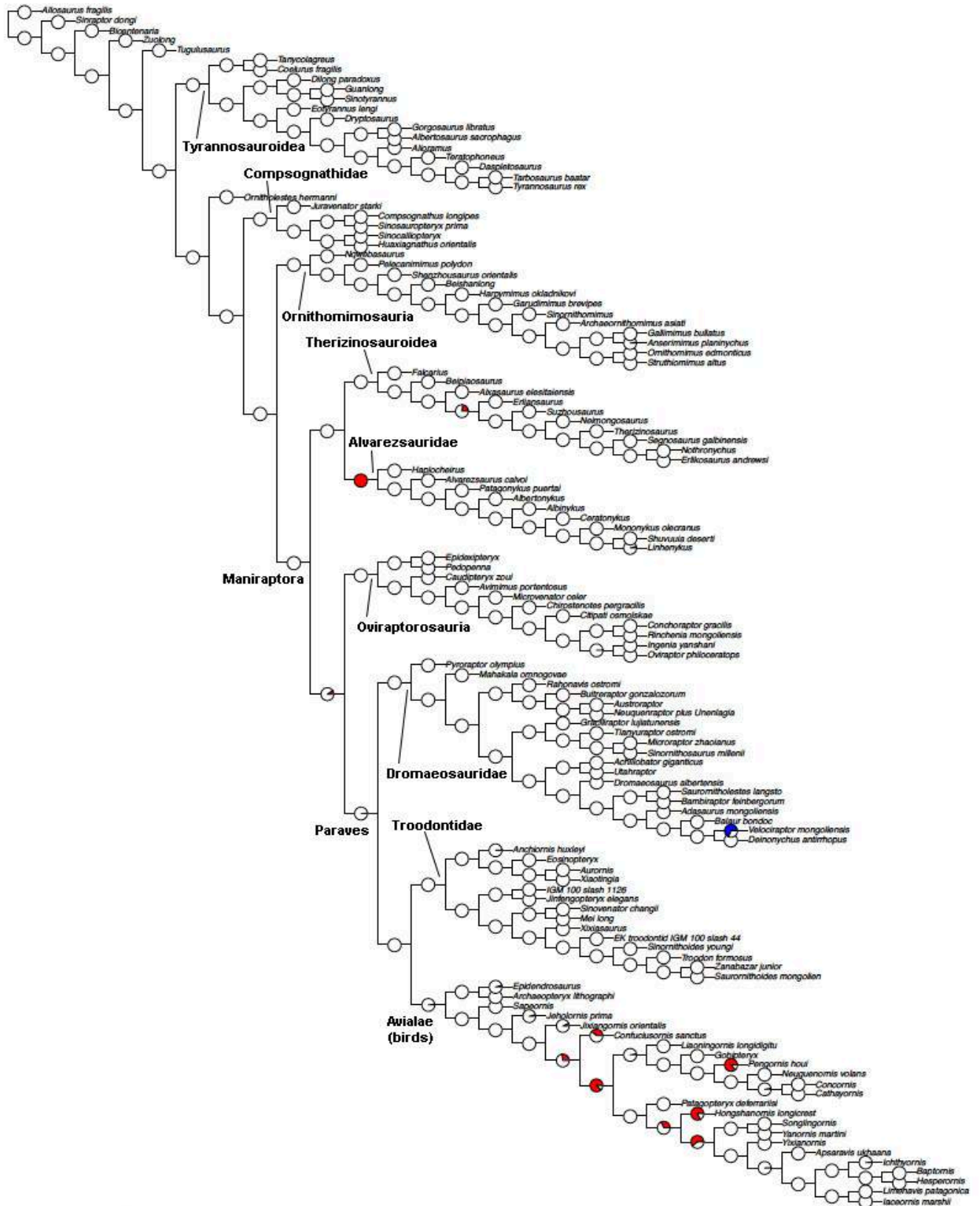


Figure 42. Disparity morphospace resulting from Principal Coordinate Analysis (PCO) for the forelimb in various coelurosaurian clades. Black squares = Tyrannosauroidae; blue asterisks = Compsognathidae; empty circles = Ornithomimosauria; blue crosses = Alvarezsauridae; pink solid circles = Oviraptorosauria; green rhombs = Therizinosauria; empty red triangles pointing up = Dromaeosauridae; empty red triangles pointing down = Troodontidae; red solid triangles = Avialae (birds).

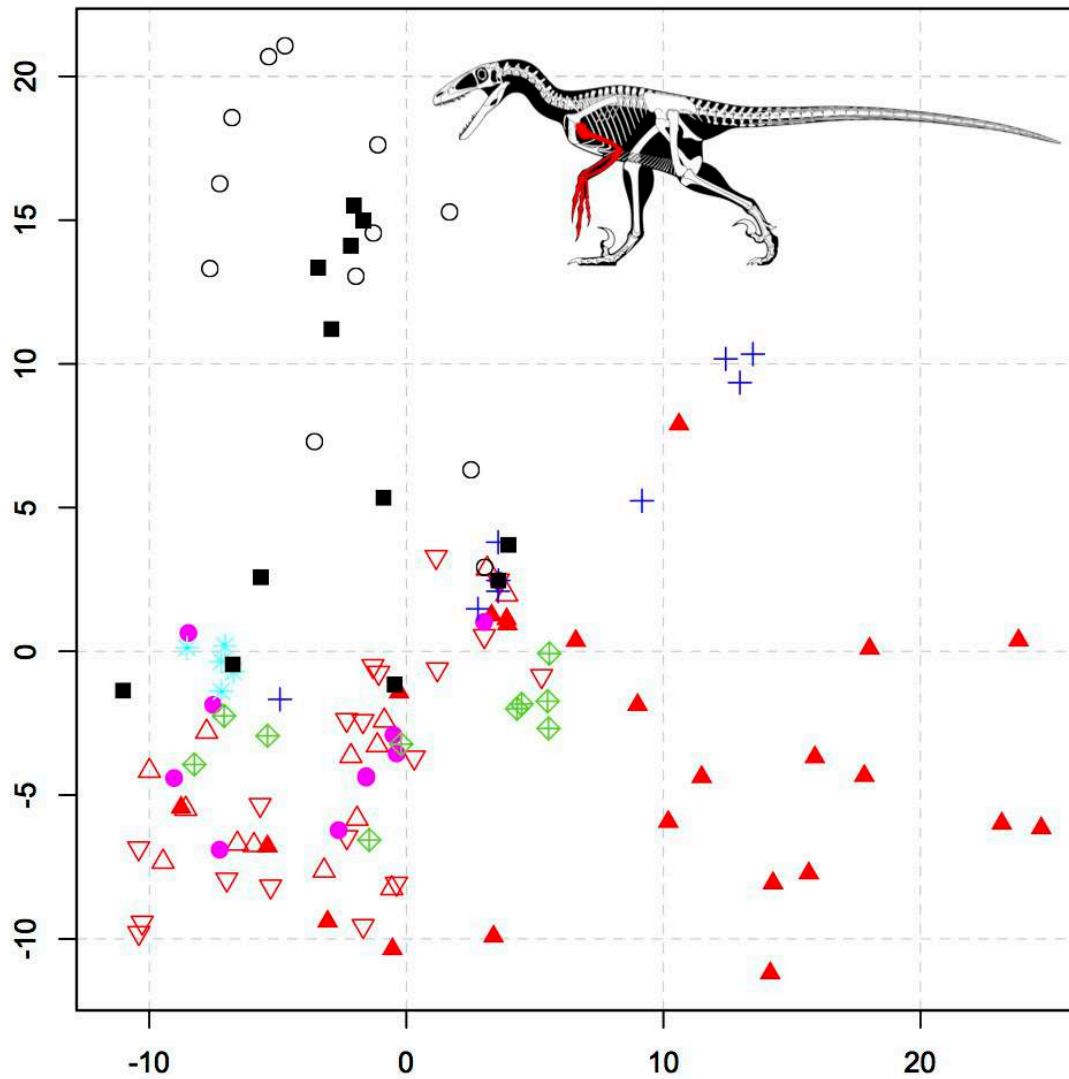


Figure 43. Forelimb disparity results based on taxa binned by clad. Disparity values based on the weighted mean pairwise disparity (WMPD) from the generalised Euclidean distance matrix (GED). 95% confidence intervals based on 10,000 bootstrap replicates are also plotted.

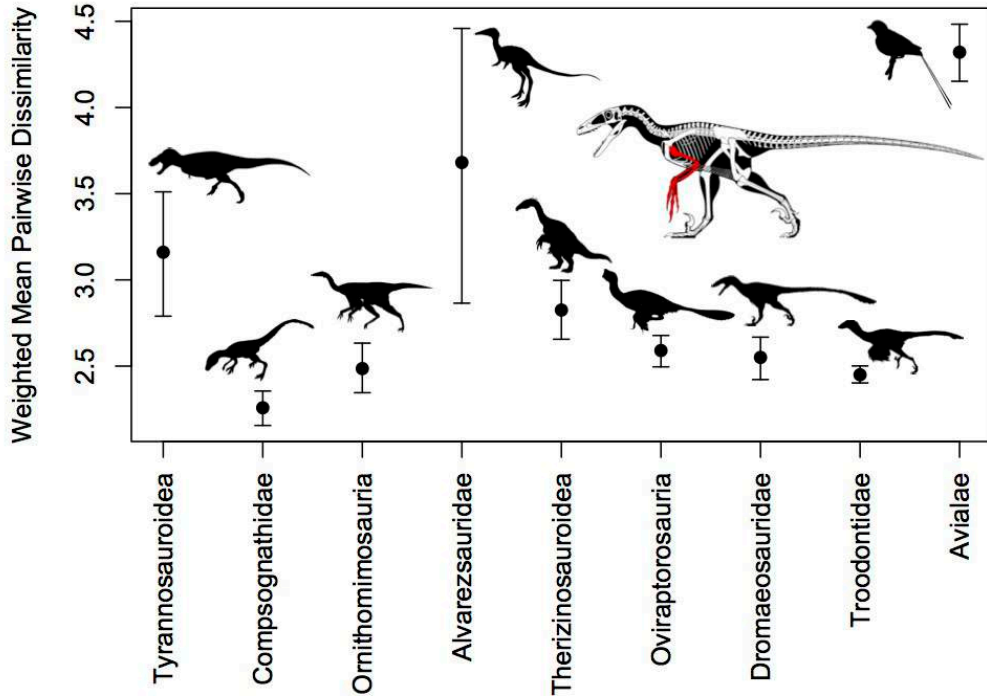


Figure 44. Forelimb disparity results based on taxa binned by clad. Disparity values based on the weighted mean pairwise disparity (WMPD) from the sum of variances from PCO scores. 95% confidence intervals based on 10,000 bootstrap replicates are also plotted.

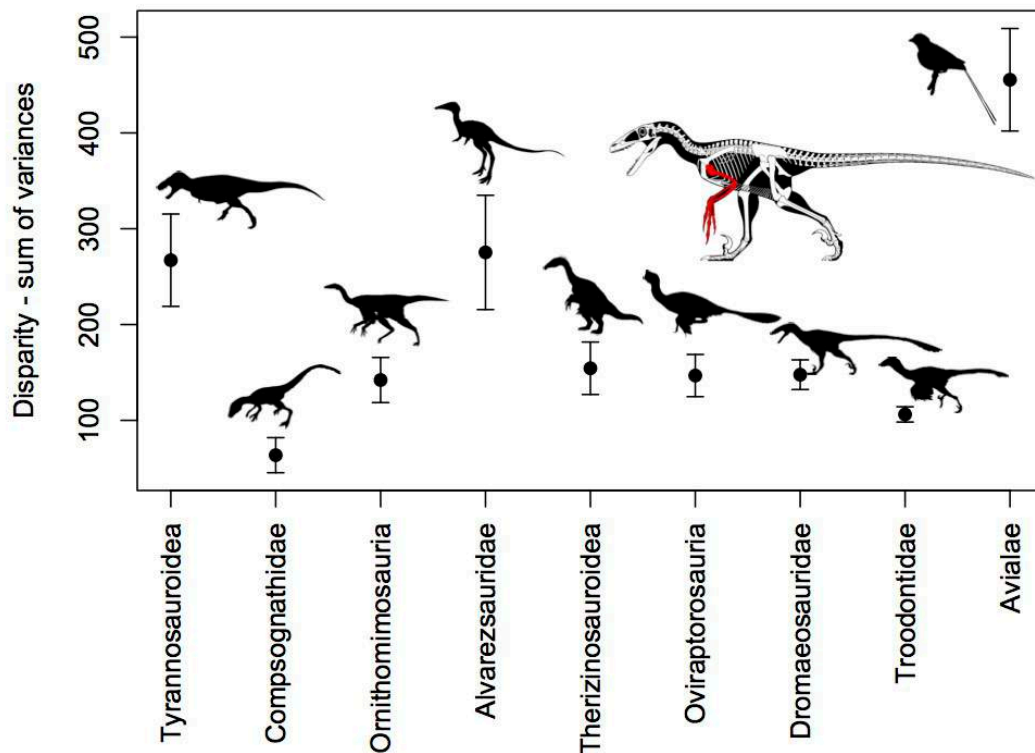


Figure 45. Temporal disparity trend of the forelimb in coelurosaurian theropods.

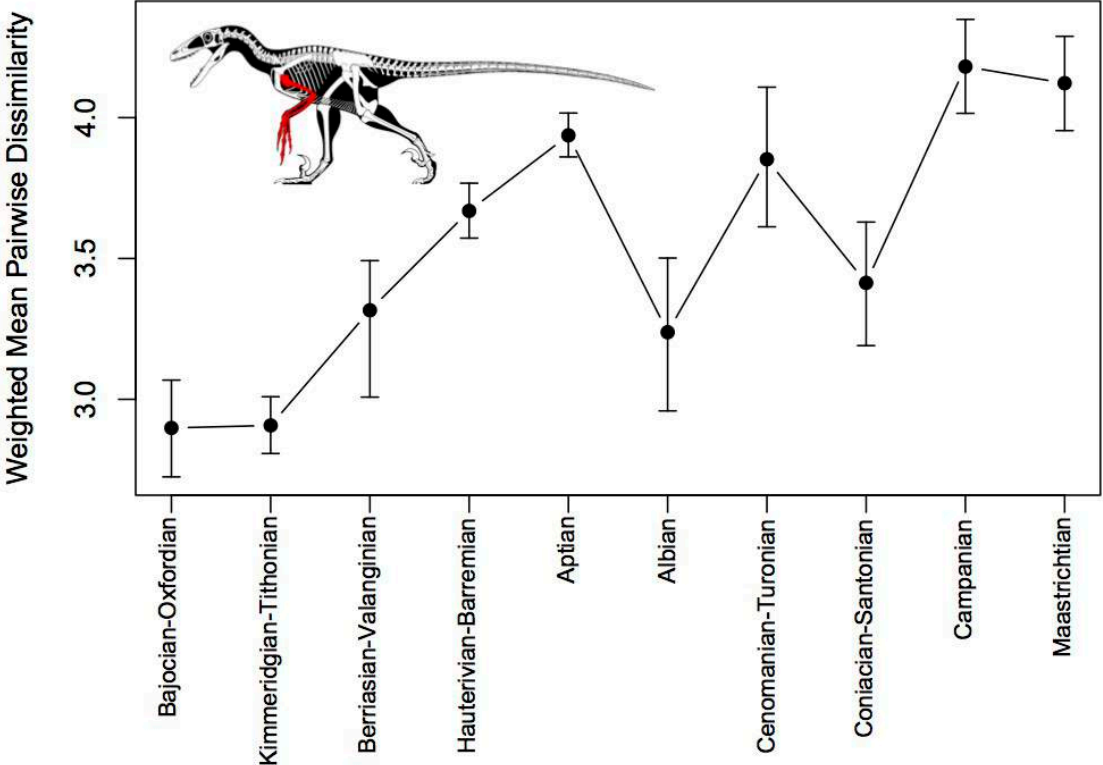


Figure 46. Rates of morphological evolution based on pelvic characters in Coelurosauria. The proportion of significantly high (red) and significantly low (blue) per-branch rates based on 100 dating replications are illustrated with pie charts.

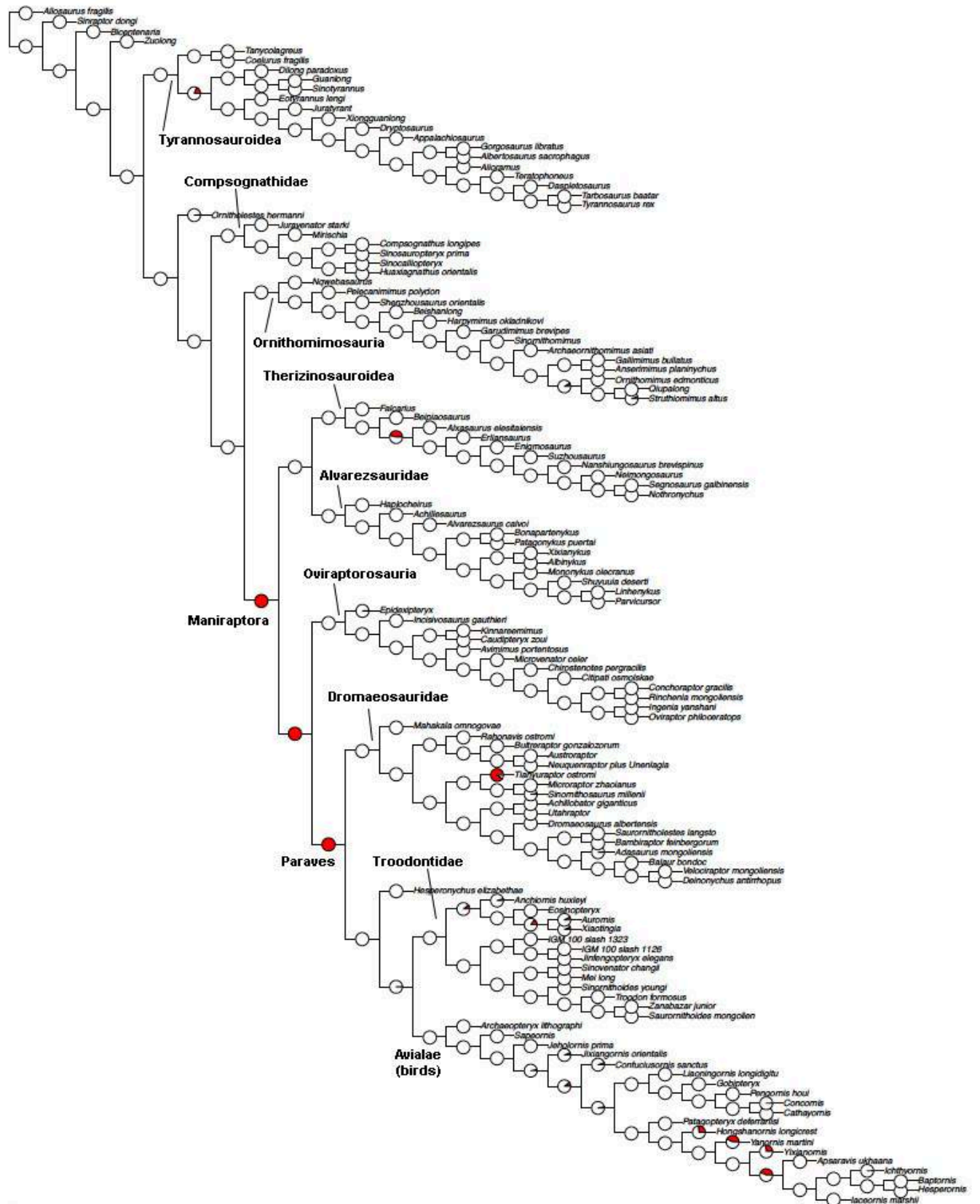


Figure 47. Disparity morphospace resulting from Principal Coordinate Analysis (PCO) for the pelvic girdle in various coelurosaurian clades. Black squares = Tyrannosauroidae; blue asterisks = Compsognathidae; empty circles = Ornithomimosauria; blue crosses = Alvarezsauridae; pink solid circles = Oviraptorosauria; green rhombs = Therizinosauria; empty red triangles pointing up = Dromaeosauridae; empty red triangles pointing down = Troodontidae; red solid triangles = Avialae (birds).

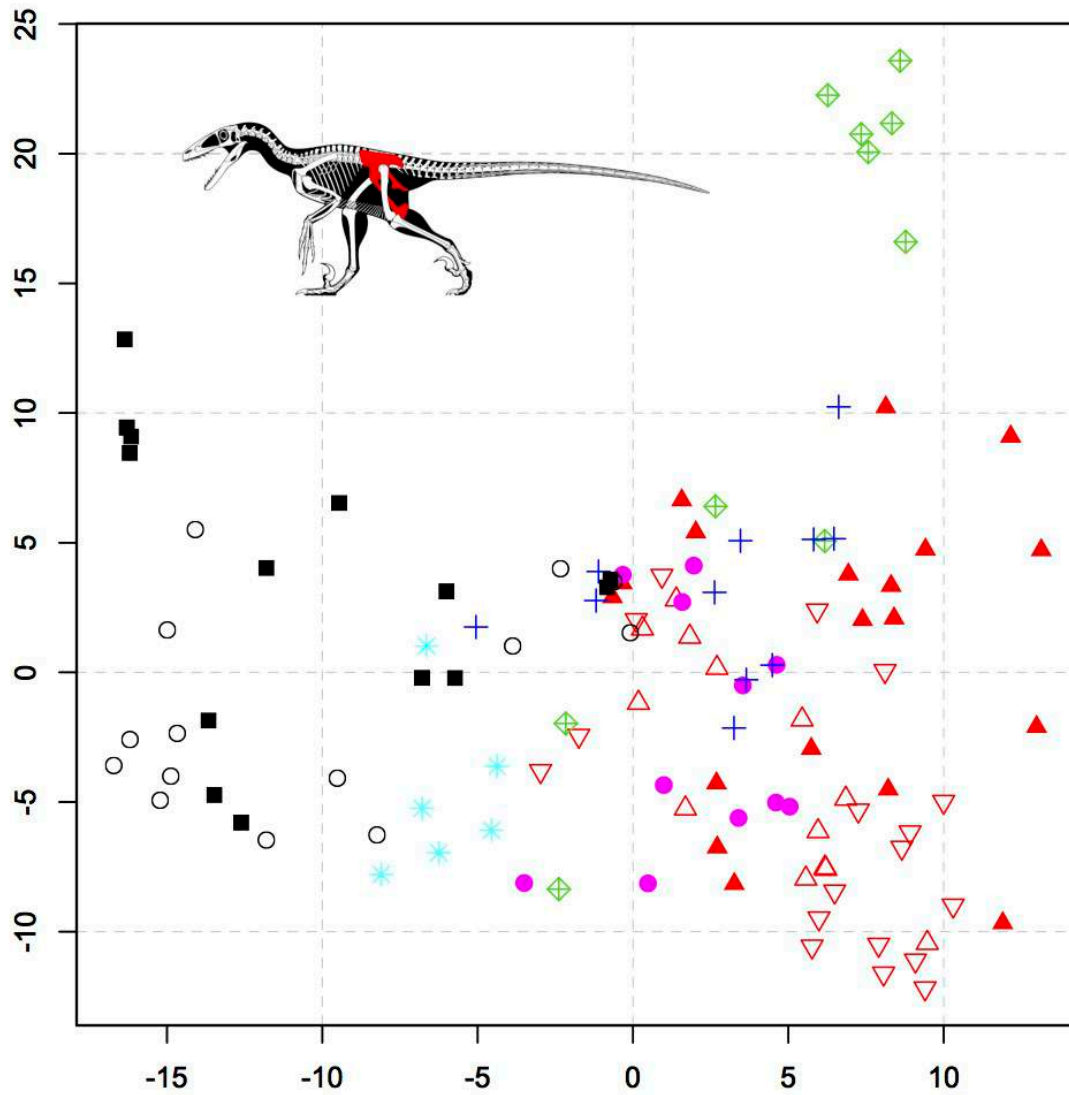


Figure 48. Pelvic disparity results based on taxa binned by clad. Disparity values based on the weighted mean pairwise disparity (WMPD) from the generalised Euclidean distance matrix (GED). 95% confidence intervals based on 10,000 bootstrap replicates are also plotted.

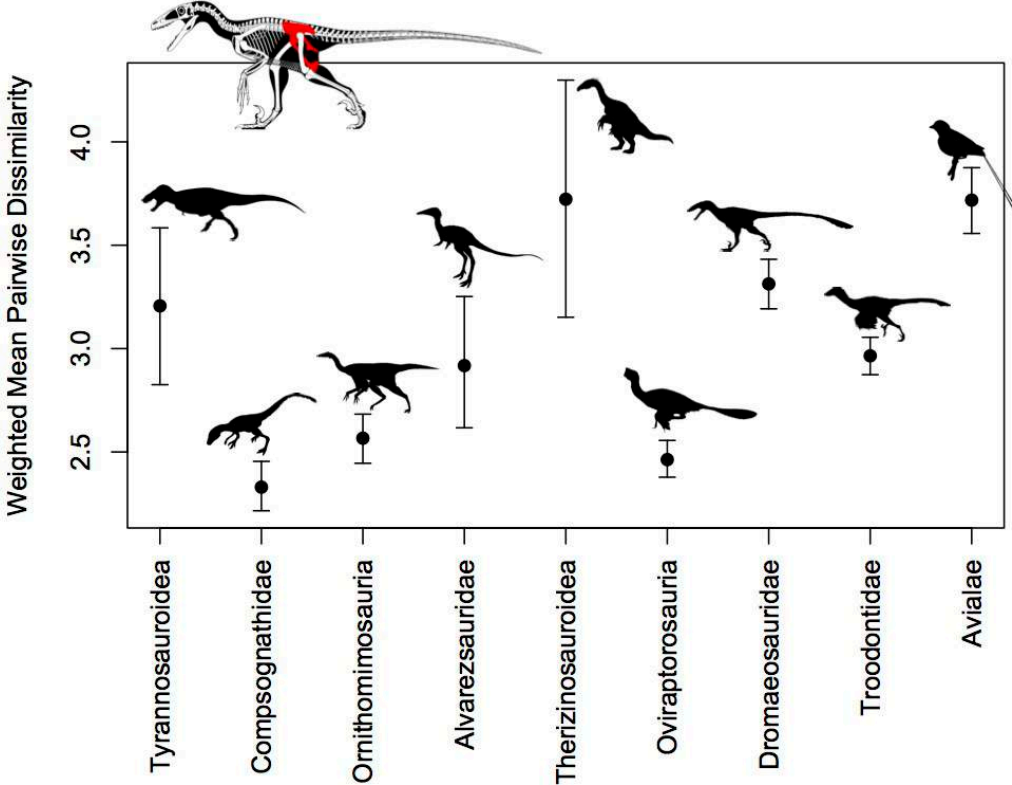


Figure 49. Pelvic disparity results based on taxa binned by clad. Disparity values based on the weighted mean pairwise disparity (WMPD) from the sum of variances from PCO scores. 95% confidence intervals based on 10,000 bootstrap replicates are also plotted.

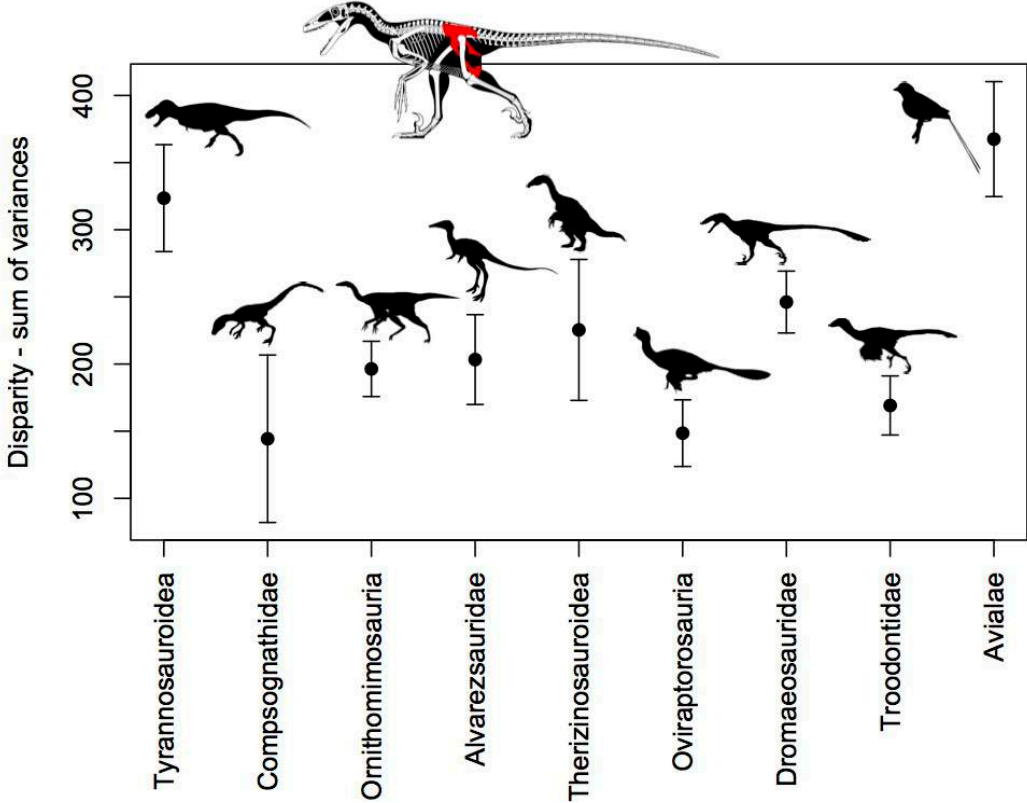


Figure 50. Temporal disparity trend of the pelvic girdle in coelurosaurian theropods.

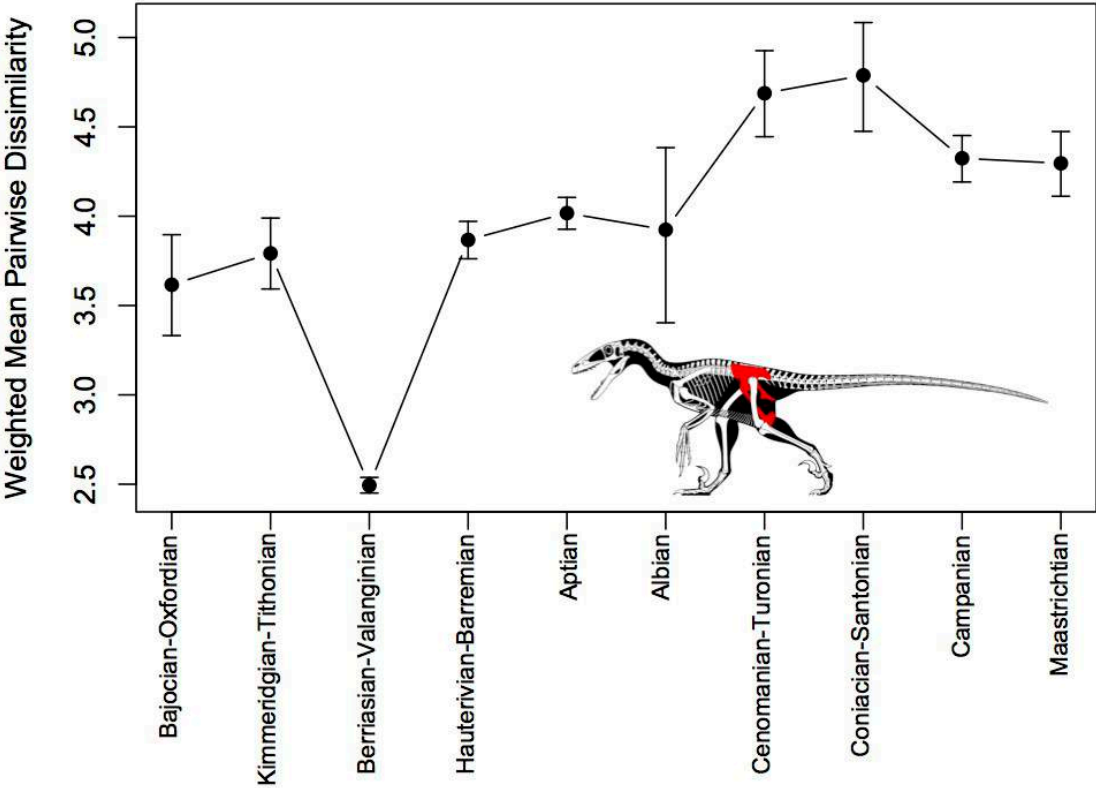


Figure 51. Rates of morphological evolution based on hindlimb characters in Coelurosauria. The proportion of significantly high (red) and significantly low (blue) per-branch rates based on 100 dating replications are illustrated with pie charts.

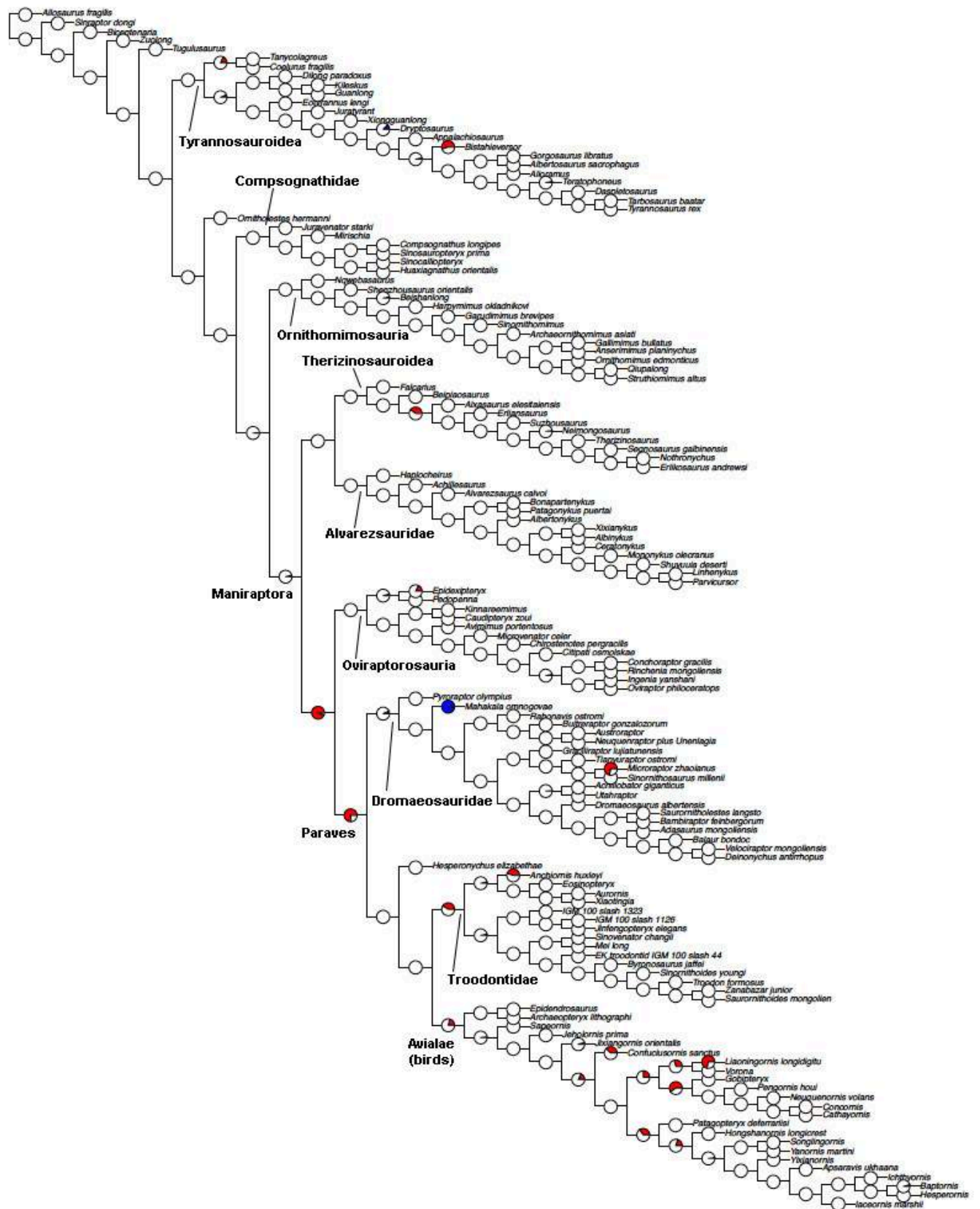


Figure 52. Disparity morphospace resulting from Principal Coordinate Analysis (PCO) for the hindlimb in various coelurosaurian clades. Black squares = Tyrannosauoidea; blue asterisks = Compsognathidae; empty circles = Ornithomimosauria; blue crosses = Alvarezsauridae; pink solid circles = Oviraptorosauria; green rhombs = Therizinosauria; empty red triangles pointing up = Dromaeosauridae; empty red triangles pointing down = Troodontidae; red solid triangles = Avialae (birds).

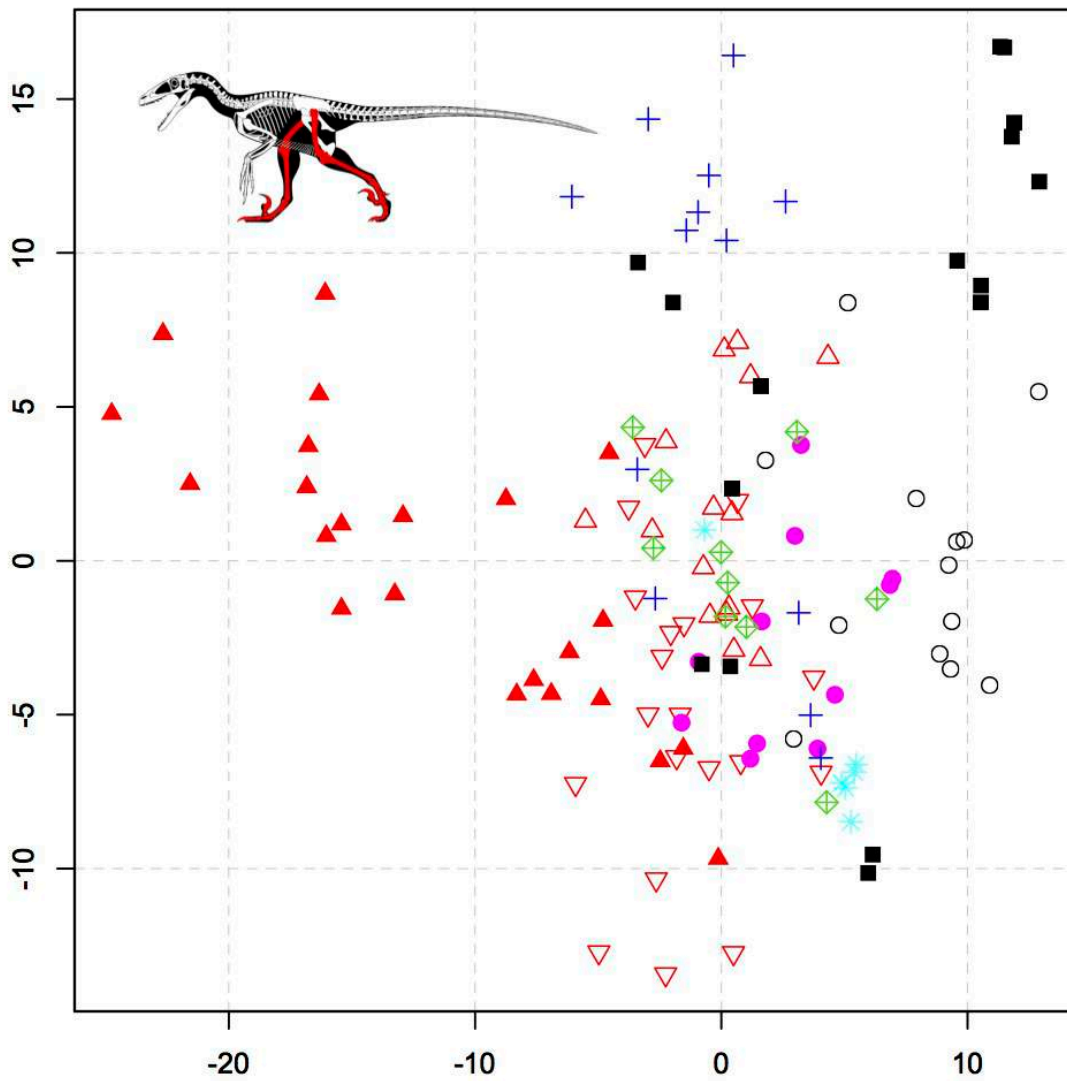


Figure 53. Hindlimb disparity results based on taxa binned by clade. Disparity values based on the weighted mean pairwise disparity (WMPD) from the generalised Euclidean distance matrix (GED). 95% confidence intervals based on 10,000 bootstrap replicates are also plotted.

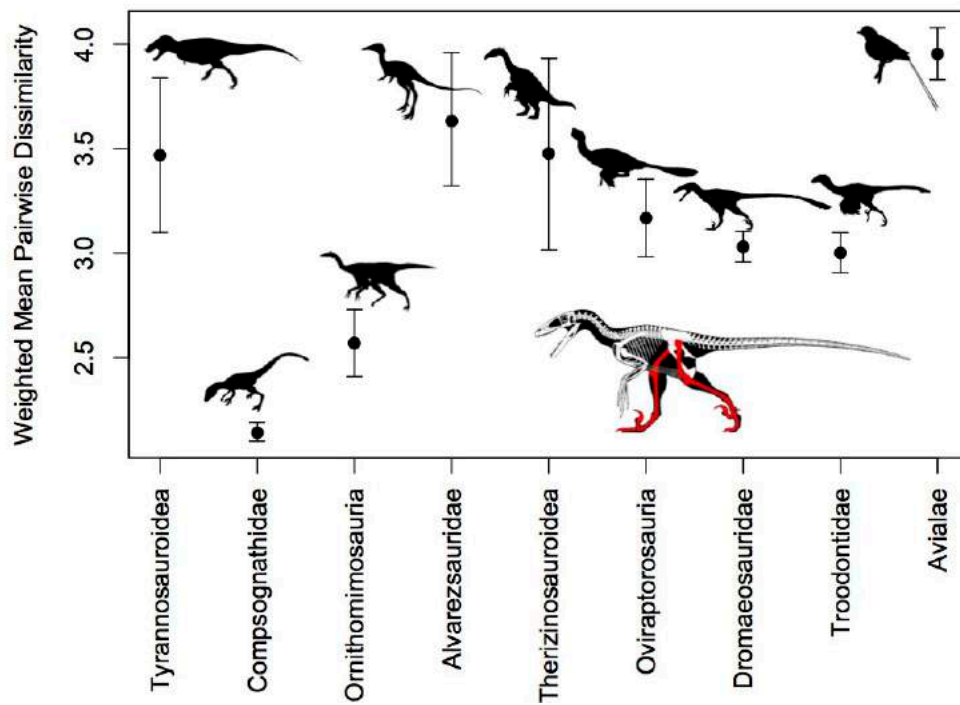


Figure 54. Hindlimb disparity results based on taxa binned by clade. Disparity values based on the weighted mean pairwise disparity (WMPD) from the sum of variances from PCO scores. 95% confidence intervals based on 10,000 bootstrap replicates are also plotted.

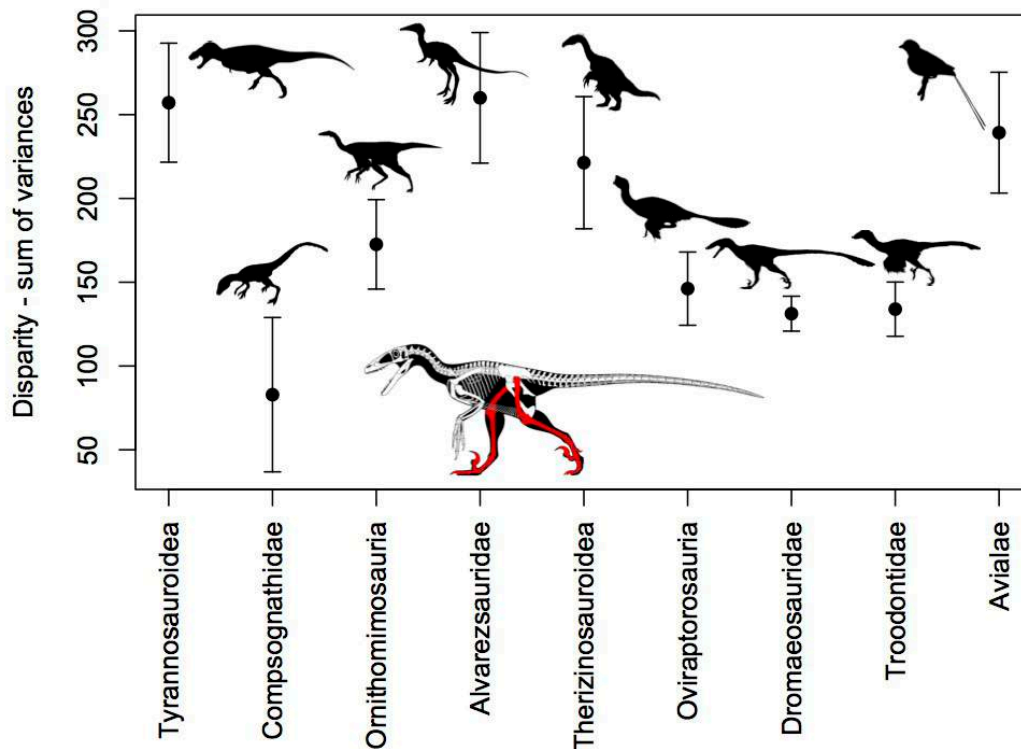


Figure 55. Temporal disparity trend of the hindlimb in coelurosaurian theropods.

